

Ion-Pairing of Phosphonium Salts in Solution: C–H⋯Halogen and C–H⋯ π Hydrogen Bonds

Johannes Ammer,* Christoph Nolte, Konstantin Karaghiosoff,* Sebastian Thallmair, Peter Mayer, Regina de Vivie-Riedle, and Herbert Mayr^[a]

Abstract: The ¹H NMR chemical shifts of the C(α)–H protons of arylmethyl triphenylphosphonium ions in CD₂Cl₂ solution strongly depend on the counteranions X[−]. The values for the benzhydryl derivatives Ph₂CH–PPh₃⁺X[−], for example, range from $\delta_{\text{H}}=8.25$ (X[−]=Cl[−]) over 6.23 (X[−]=BF₄[−]) to 5.72 ppm (X[−]=BPh₄[−]). Similar, albeit weaker, counterion-induced shifts are observed for the *ortho*-protons of all aryl groups. Concentration-dependent NMR studies show that the large shifts result from the deshielding of the protons by the anions, which decreases in the order Cl[−] > Br[−] ≫ BF₄[−] > SbF₆[−]. For the less bulky derivatives PhCH₂–PPh₃⁺X[−], we also find C–H⋯Ph interactions between C(α)–H and a phenyl

group of the BPh₄[−] anion, which result in upfield NMR chemical shifts of the C(α)–H protons. These interactions could also be observed in crystals of (*p*-CF₃-C₆H₄)CH₂–PPh₃⁺BPh₄[−]. However, the dominant effects causing the counterion-induced shifts in the NMR spectra are the C–H⋯X[−] hydrogen bonds between the phosphonium ion and anions, in particular Cl[−] or Br[−]. This observation contradicts earlier interpretations which assigned these shifts predominantly to the ring current of the BPh₄[−] anions. The concentration

dependence of the ¹H NMR chemical shifts allowed us to determine the dissociation constants of the phosphonium salts in CD₂Cl₂ solution. The cation–anion interactions increase with the acidity of the C(α)–H protons and the basicity of the anion. The existence of C–H⋯X[−] hydrogen bonds between the cations and anions is confirmed by quantum chemical calculations of the ion pair structures, as well as by X-ray analyses of the crystals. The IR spectra of the Cl[−] and Br[−] salts in CD₂Cl₂ solution show strong red-shifts of the C–H stretch bands. The C–H stretch bands of the tetrafluoroborate salt PhCH₂–PPh₃⁺BF₄[−] in CD₂Cl₂, however, show a blue-shift compared to the corresponding BPh₄[−] salt.

Keywords: crystal structure • hydrogen bonds • ion pairs • NMR spectroscopy • solution structure

Introduction

Hydrogen bonds involving C–H donors have attracted considerable interest in the last two decades,^[1–3] and only recently it became generally recognized that, in many cases, these interactions have to be classified as moderate or even strong hydrogen bonds.^[4]

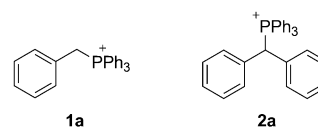
The C(α)–H protons of alkyl triphenylphosphonium salts are particularly acidic^[5,6] so that C(α)–H⋯X[−] hydrogen bonds between the phosphonium ion and its counterion X[−] should be quite favorable. The importance of such hydrogen bonds in crystals as well as in solutions of phosphonium halides was already demonstrated in a 1964 report that received only little attention.^[7] For example, the CH₂ stretching vibrations of PhCH₂–PPh₃⁺Cl[−] (**1a**Cl[−], Scheme 1) in chloroform solution (2853 and 2780 cm^{−1}) are red-shifted

($\Delta\bar{\nu} \approx -80$ cm^{−1}) compared with those of the corresponding BPh₄[−] salt (2937 and 2857 cm^{−1}). Likewise, the CH₂ signals in the ¹H NMR spectrum of **1a**Cl[−] were reported to be shifted downfield relative to those of **1a**BPh₄[−] ($\Delta\delta_{\text{H}} \approx +0.4$ ppm in CH₃CN).^[7] Spectral shifts as those observed for **1a**Cl[−] are classical criteria for a hydrogen bond.^[8]

Schiemenz and co-workers have collected an enormous wealth of data on ¹H NMR spectra of phosphonium salts and found analogous trends, that is, that the α protons of phosphonium ions in chloroform or dichloromethane solution generally undergo upfield shifts of up to $\Delta\delta_{\text{H}} \approx -3$ ppm when the counterion is exchanged from halide to BPh₄[−].^[9,10] Similar results were found for other onium salts.^[11–15] According to these reports, the interaction between the onium ions and “normal” inorganic anions such as halide ions plays only a minor role and is related to the phenomenon of solvation.^[9] Instead, the large upfield shifts in the BPh₄[−] salts (e.g., $\Delta\delta_{\text{H}} = -1.41$ ppm for **1a**BPh₄[−] compared to **1a**Br[−] in

[a] Dr. J. Ammer, Dr. C. Nolte, Prof. Dr. K. Karaghiosoff, S. Thallmair, Dr. P. Mayer, Prof. Dr. R. de Vivie-Riedle, Prof. Dr. H. Mayr
Ludwig-Maximilians-Universität München, Butenandtstrasse 5–13
81377 München (Germany)
Fax: (+49) 89-2180-77398
E-mail: Johannes.Ammer@cup.uni-muenchen.de
Konstantin.Karaghiosoff@cup.uni-muenchen.de

Supporting information for this article is available on the WWW under <http://dx.doi.org/10.1002/chem.201204561>.



Scheme 1. Structures of the phosphonium ions **1a** and **2a**.

CD₂Cl₂)^[9] were rationalized to be predominantly caused by the ring current of the BPh₄⁻ anion's phenyl rings, which reside above the C(α)-H protons of the phosphonium ion due to Coulomb attraction between the two ions.^[9,10,16,17] Based on this effect, many applications of the BPh₄⁻ anion as shift reagent in NMR spectroscopy have been described.^[9,11–15,18]

One of the examples used by Schiemenz to illustrate the usefulness of the “BPh₄⁻ effect” was the possibility to determine ²J_{H,P} for the α proton of Ph₂CH–PPh₃⁺ (**2a**).^[9] This could not be achieved in the absence of BPh₄⁻ due to the overlap of the C(α)-H signals with the aromatic protons in the NMR spectra of the corresponding halide salts. In the course of our studies of phosphonium salts as precursors for the photogeneration of carbocations,^[19,20] we required knowledge about the ion pairing of the phosphonium salt **2aX**⁻ in solution. Much to our surprise, our data clearly showed that the C(α)-H protons of **2aBPh**₄⁻ do not experience any significant ring current effect in CD₂Cl₂ solution. Considering the relevance of phosphonium ion/anion interactions in crystal engineering,^[21] anion recognition,^[22] salt-based solvent systems,^[23,24] photochemistry,^[19,20,25] structure determination,^[10,26] and organic synthesis,^[27,28] we decided to carry out a more detailed investigation of the ion pairing in **2aX**⁻ and related phosphonium salts.

NMR Spectroscopy

¹H NMR Signals for the C(α)-H protons of phosphonium salts in CD₂Cl₂ solution

Benzhydryl triphenylphosphonium salts (2aX⁻): Ion pairing of the salts Ph₂CH–PPh₃⁺ X⁻ (**2aX**⁻) in CD₂Cl₂ solution is

evident from the fact that the NMR spectra of **2a** depend on the counterion X⁻ (Table 1). The most obvious effect is the large change of the ¹H NMR chemical shifts (Δδ_H = +2.53 ppm) for the C(α)-H protons (CHP⁺) when X⁻ is varied from BPh₄⁻ via SbF₆⁻, BF₄⁻, and Br⁻ to Cl⁻ (Table 1).

Figure 1 shows that the δ_H values of the C(α)-H protons of **2aBPh**₄⁻ in CD₂Cl₂ are almost independent of the salt concentration (δ_H ≈ 5.78 ppm, Table 2). Moreover, the values for **2aBPh**₄⁻ differ by only 0.2 ppm or less from those of **2aSbF**₆⁻. These observations clearly rule out any significant influence of the ring current of the BPh₄⁻ anions' phenyl rings on the chemical shifts of the C(α)-H protons of **2a**, as suggested by Schiemenz.^[9]

At concentrations of [**2aX**⁻] > 0.02 M, the δ_H values of the C(α)-H protons of **2aX**⁻ with X⁻ = Cl⁻, Br⁻, BF₄⁻, or SbF₆⁻ reach plateaus (Figure 1) and we can conclude that at

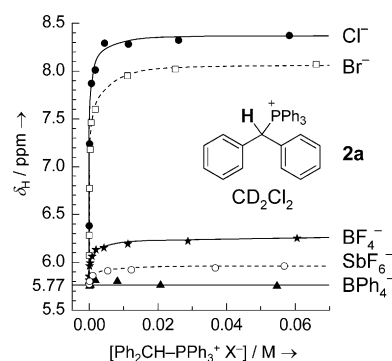


Figure 1. Concentration-dependent ¹H NMR (600 MHz, 27°C) chemical shifts δ_H of the benzylic C(α)-H protons of **2aX**⁻ with different counter-anions X⁻ = Cl⁻ (●), Br⁻ (□), BF₄⁻ (★), SbF₆⁻ (○), or BPh₄⁻ (▲) in CD₂Cl₂.

Table 1. ³¹P NMR (162 MHz), ¹H NMR (400 MHz), and ¹³C NMR (100 MHz) data for the phosphonium ion **2a** in CD₂Cl₂. Data for **2aX**⁻ were determined at concentrations where the phosphonium salts exist as ion pairs.

Salt	P ⁺ δ _P [ppm]	CHP ⁺		<i>o</i> -CHPh ₂ δ _H [ppm]	<i>m</i> -CHPh ₂ δ _H [ppm]	<i>p</i> -CHPh ₂ δ _H [ppm]	<i>o</i> -PPh ₃ δ _H [ppm]	<i>m</i> -PPh ₃ δ _H [ppm]	<i>p</i> -PPh ₃ δ _H [ppm]
		δ _H [ppm] (² J _{H,P} [Hz])	¹ J _{H,C} ^[a] [Hz]						
2aCl ⁻	22.1	8.25 (18.3)	131.3	7.55–7.60 ^[b]	7.20–7.30 ^[b]	7.20–7.30 ^[b]	7.79–7.84	7.55–7.60 ^[b]	7.72–7.77
2aBr ⁻	22.1	8.10 (18.0)	131.1	7.53–7.61 ^[b]	7.21–7.31 ^[b]	7.21–7.31 ^[b]	7.74–7.79 ^[b]	7.53–7.61 ^[b]	7.74–7.79 ^[b]
2aBF ₄ ⁻	21.8	6.23 (17.4)	130.2	7.19–7.22	7.28–7.33	7.35–7.40	7.43–7.49	7.59–7.65	7.81–7.85
2aSbF ₆ ⁻	21.7	5.98 (17.2)	129.3	7.15–7.17	7.30–7.34	7.38–7.44 ^[b]	7.38–7.44 ^[b]	7.61–7.66	7.82–7.87
2aBPh ₄ ⁻	21.6	5.72 (17.1)	128.7	7.05–7.10	7.27–7.36 ^[c]	7.39–7.47	7.27–7.36 ^[c]	7.55–7.62	7.79–7.86
“free” 2a ^[d]	–	5.77 (17.0)	– ^[e]	7.09–7.11	7.33–7.37 ^[b]	7.42–7.45	7.33–7.37 ^[b]	7.62–7.65	7.85–7.89
Δ(Cl ⁻) ^[f]	+0.6	+2.53 (+1.2)	+2.6	~+0.50	~–0.07	~–0.18	~+0.50	~±0	~–0.08
Salt	CHP ⁺ δ _C [ppm] (¹ J _{C,P} [Hz])	<i>i</i> -CHPh ₂ δ _C [ppm] (² J _{C,P} [Hz])	<i>o</i> -CHPh ₂ δ _C [ppm] (³ J _{C,P} [Hz])	<i>m</i> -CHPh ₂ δ _C [ppm] (⁴ J _{C,P} [Hz])	<i>p</i> -CHPh ₂ δ _C [ppm] (⁵ J _{C,P} [Hz])	<i>i</i> -PPh ₃ δ _C [ppm] (¹ J _{C,P} [Hz])	<i>o</i> -PPh ₃ δ _C [ppm] (² J _{C,P} [Hz])	<i>m</i> -PPh ₃ δ _C [ppm] (³ J _{C,P} [Hz])	<i>p</i> -PPh ₃ δ _C [ppm] (⁴ J _{C,P} [Hz])
2aCl ⁻	45.3 (41.8)	134.3 (4.0)	131.7 (6.9)	129.4 (1.5)	129.0 (2.7)	119.2 (82.3)	135.7 (9.2)	130.3 (12.3)	135.2 (3.1)
2aBr ⁻	45.9 (42.3)	134.1 (4.0)	131.6 (6.8)	129.5 (1.7)	129.2 (2.5)	119.0 (82.4)	135.7 (9.3)	130.3 (12.4)	135.3 (3.1)
2aBF ₄ ⁻	49.6 (43.9)	132.9 (4.1)	131.1 (6.6)	130.0 (1.7)	129.9 (2.6)	118.3 (82.5)	135.3 (9.1)	130.8 (12.4)	135.9 (3.1)
2aSbF ₆ ⁻	50.5 (44.2)	132.6 (4.2)	130.9 (6.6)	130.1 (1.8)	130.0 (2.5)	118.1 (82.7)	135.2 (9.1)	130.8 (12.4)	136.0 (3.1)
2aBPh ₄ ⁻	51.3 (44.3)	132.3 (4.2)	130.8 (6.6)	130.25 (1.7)	130.32 (2.5)	117.9 (82.6)	135.2 (9.1)	131.0 (12.2)	136.3 (3.1)
Δ(Cl ⁻) ^[f]	–6.0 (–2.5)	+2.0 (–0.2)	+0.9 (+0.3)	–0.8 (–0.2)	–1.3 (+0.2)	+1.3 (–0.3)	+0.5 (+0.1)	–0.7 (+0.1)	–1.1 (±0)

[a] ¹J_{H,C} determined from ¹³C satellites in the ¹H NMR (600 MHz) spectra. [b] Two signals superimposed. [c] Superimposed with *o*-protons of BPh₄⁻. [d] ¹H NMR (600 MHz) spectrum of a 2.13 × 10⁻⁵ M solution of **2a** SbF₆⁻ in CD₂Cl₂. At this concentration, the phosphonium salt predominantly exists in the form of the free (unpaired) ions. [e] Not available. [f] Difference between **2aCl**⁻ and **2aBPh**₄⁻ (the latter has virtually the same ¹H NMR spectrum as “free” **2a**).

Table 2. Concentration-dependent ^1H NMR chemical shifts δ_{H} (600 MHz) for C(α)-H and dissociation constants K_{D} [M] of **2a** X^- with different counterions X^- in CD_2Cl_2 .

Salt	$[\mathbf{2aX}^-]/\text{M}$	δ_{H} [ppm]	$x_{\text{paired,exptl}}$	$K_{\text{D}}^{[\text{a}]}$ [M]	$x_{\text{paired,calcd}}^{[\text{b}]}$
2a BPh_4^-	1.75×10^{-5}	5.80	–	–	–
	1.03×10^{-4}	5.75	–	–	–
	4.07×10^{-4}	5.76	–	–	–
	1.76×10^{-3}	5.81	–	–	–
	8.25×10^{-3}	5.80	–	–	–
	2.08×10^{-2}	5.76	–	–	–
	5.47×10^{-2}	5.75	–	–	–
	average δ_{H}	5.78			
2a SbF_6^-	2.13×10^{-5}	5.77	0.00		0.03
	1.07×10^{-4}	5.80	0.16		0.13
	1.02×10^{-3}	5.86	0.47	6×10^{-4}	(0.47)
	5.44×10^{-3}	5.91	0.74		0.72
	1.23×10^{-2}	5.92	0.79		0.80
	3.68×10^{-2}	5.94	0.89		0.88
	5.68×10^{-2}	5.96	1.00		0.90
	2.12×10^{-5}	5.81	0.08		0.08
2a BF_4^-	4.22×10^{-5}	5.85	0.17		0.14
	1.03×10^{-4}	5.96	0.40		0.26
	3.36×10^{-4}	5.99	0.46	2.2×10^{-4}	(0.46)
	8.91×10^{-4}	6.06	0.60		0.61
	2.01×10^{-3}	6.13	0.75		0.72
	4.26×10^{-3}	6.15	0.79		0.80
	1.13×10^{-2}	6.19	0.88		0.87
	2.87×10^{-2}	6.22	0.94		0.92
2a Br^-	6.06×10^{-2}	6.25	1.00		0.94
	1.81×10^{-5}	6.07	0.13		0.17
	3.58×10^{-5}	6.28	0.22		0.26
	1.03×10^{-4}	6.77	0.43	7.6×10^{-5}	(0.43)
	3.04×10^{-4}	7.18	0.61		0.61
	6.09×10^{-4}	7.46	0.73		0.70
	1.83×10^{-3}	7.6 ^[c]	0.80		0.82
	1.12×10^{-2}	7.95	0.95		0.92
2a Cl^-	2.51×10^{-2}	8.02	0.98		0.95
	6.62×10^{-2}	8.07	1.00		0.97
	2.31×10^{-5}	6.38	0.23		0.32
	1.00×10^{-4}	7.24	0.57	3.4×10^{-5}	(0.57)
	7.13×10^{-4}	7.87	0.81		0.81
	1.76×10^{-3}	8.01	0.86		0.87
	4.45×10^{-3}	8.29	0.97		0.92
	1.14×10^{-2}	8.28	0.97		0.95
	2.61×10^{-2}	8.32	0.98		0.96
	5.83×10^{-2}	8.37	1.00		0.98

[a] K_{D} derived from the data for phosphonium salt concentrations where $x_{\text{paired,exptl}} \approx 0.5$. [b] Calculated using K_{D} from this table. [c] Superimposed with signals of aryl protons.

these concentrations we observe ion pairs almost exclusively. Literature NMR spectra of phosphonium salts in CD_2Cl_2 or CDCl_3 solution, which were recorded under typical conditions of NMR measurements, can thus be expected to characterize the ion pairs.

At lower concentrations ($< 5 \times 10^{-3} \text{ M}$), the chemical shifts of the C(α)-H protons of **2a** X^- with all investigated anions except BPh_4^- decrease markedly and approach δ_{H} of the tetraphenylborate salt (Figure 1). Finally, at a concentration of $2.13 \times 10^{-5} \text{ M}$, the chemical shift of the C(α)-H proton of **2aSbF₆⁻** reaches a value of $\delta_{\text{H}} = 5.77 \text{ ppm}$ (Table 2), which is identical to δ_{H} observed for **2aBPh₄⁻**. We can therefore assume that this δ_{H} value corresponds to the unpaired

$\text{Ph}_2\text{CH}-\text{PPh}_3^+$ ions (**2a**). The determination of the K_{D} values listed in Table 2 will be discussed below.

Benzyl triphenylphosphonium salts (1a,bX⁻): It was already noted by Schiemenz and co-workers, that the “ BPh_4^- effect” decreases with steric shielding.^[9,10] For that reason, we also tested the “ BPh_4^- effect” in sterically less hindered systems and investigated the concentration-dependent effects of the counteranions on the ^1H NMR chemical shifts δ_{H} (600 MHz, CD_2Cl_2) of the C(α)-H protons of the benzyl triphenylphosphonium ions $\text{PhCH}_2-\text{PPh}_3^+$ (**1a**) and the 4-(trifluoromethyl)benzyl triphenylphosphonium ions ($p\text{-CF}_3\text{-C}_6\text{H}_4\text{CH}_2-\text{PPh}_3^+$ (**1b**)) (Tables S1 and S2 in the Supporting Information). Figure 2a and b illustrate the data.

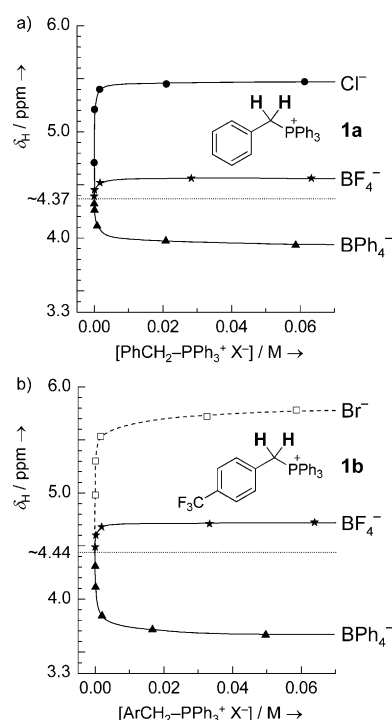


Figure 2. Concentration-dependent ^1H NMR (600 MHz, 27°C) chemical shifts δ_{H} of the benzylic C(α)-H protons of a) **1a** X^- or b) **1b** X^- with different counteranions $\text{X}^- = \text{Cl}^-$ (●), Br^- (□), BF_4^- (★), or BPh_4^- (▲) in CD_2Cl_2 .

The phosphonium halides **1aCl⁻** and **1bBr⁻**, as well as the tetrafluoroborates **1a,bBF₄⁻**, show similar behavior as the corresponding benzhydryl triphenylphosphonium salts **2a** X^- . In the concentration range $[\mathbf{1a,bX}^-] \geq 0.02 \text{ M}$, the δ_{H} values of the C(α)-H protons are virtually constant and we can conclude that the phosphonium halides and tetrafluoroborates predominantly exist as ion pairs under these conditions (Figure 2). At lower concentrations ($< 5 \times 10^{-3} \text{ M}$), the δ_{H} values decrease: For $2 \times 10^{-5} \text{ M}$ solutions of the tetrafluoroborate salts, we determined chemical shifts of $\delta_{\text{H}} = 4.39$ (**1aBF₄⁻**) and 4.49 ppm (**1bBF₄⁻**) for the C(α)-H protons (Tables S1 and S2 in the Supporting Information).

The C(α)-H protons of the tetraphenylborate salts **1a**, **b** BPh₄⁻, however, show the opposite effect: Their chemical shifts are also virtually constant (**1a** BPh₄⁻: 3.95 ppm; **1b** BPh₄⁻: 3.68 ppm) at concentrations ≥ 0.02 M, but increase with decreasing concentration until they reach the value of $\delta_{\text{H}} = 4.32$ ppm (**1a** BPh₄⁻) or 4.31 ppm (**1b** BPh₄⁻) at concentrations of 2×10^{-5} M (Figure 2).

Thus, the δ_{H} values of the C(α)-H protons of **1a**X⁻ with different counteranions X⁻ approach a common value of $4.32 < \delta_{\text{H}} < 4.39$ ppm at low concentrations of **1a**X⁻, and we can estimate $\delta_{\text{H,unpaired}} \approx 4.37$ ppm for the C(α)-H protons of the free benzyl triphenylphosphonium ion **1a**. Analogously, $4.31 < \delta_{\text{H}} < 4.49$ ppm at low concentrations of **1b**X⁻ leads to an estimate of $\delta_{\text{H,unpaired}} \approx 4.44$ ppm for the C(α)-H protons of free **1b**.

The knowledge of δ_{H} for the unpaired phosphonium ions **1a**, **b** allows us to directly compare the magnitude of the “BPh₄⁻ effect” with the influence of C(α)-H...halide hydrogen bonding. The large difference between the C(α)-H protons of the ion pairs **1a**Cl⁻ and **1a**BPh₄⁻ ($\Delta\delta_{\text{H}} = +1.54$ ppm) is mostly due to the deshielding effect of Cl⁻, whereas the shielding effect of BPh₄⁻ contributes less than 30% to the observed $\Delta\delta_{\text{H}}$. The smaller deshielding effects of the “normal” anions X⁻ = Cl⁻ and BF₄⁻ on the C(α)-H protons of **1a** (e.g., $\Delta\delta_{\text{H}} \approx +1.0$ ppm for **1a**Cl⁻ relative to unpaired **1a**) compared to those for the analogous benzhydryl derivatives **2a**X⁻ (e.g., $\Delta\delta_{\text{H}} \approx +2.5$ ppm for **2a**Cl⁻ relative to unpaired **2a**) are explained by the statistical factor of two C(α)-H protons in **1a** (vs one in **2a**) and the lower C(α)-H acidity of **1a** ($\text{p}K_{\text{a}} 17.6$ in DMSO)^[6] compared to that of **2a** ($\text{p}K_{\text{a}} \approx 9$ in DMSO estimated from the correlation equation published in ref. [5] and $\text{p}K_{\text{a}} 30.6$ for Ph₂CH₂^[29]).

The *p*-CF₃ substituent decreases the $\text{p}K_{\text{a}}$ value of the phosphonium salt **1b** in DMSO to 14.6, compared to $\text{p}K_{\text{a}} 17.6$ for the parent compound **1a**,^[6] which results in stronger C-H...X⁻ hydrogen bonds in the **1b**X⁻ ion pairs. Accordingly, Figure 2b shows comparably large downfield shifts for the C(α)-H protons in the **1b**Br⁻ and **1b**BF₄⁻ ion pairs. The “BPh₄⁻ effect” also increases with the C(α)-H acidity: The upfield shift of $\Delta\delta_{\text{H}} \approx -0.78$ ppm for the C(α)-H protons of **1b** that results from ion pairing with the BPh₄⁻ ion is almost twice as large as the upfield shift of $\Delta\delta_{\text{H}} \approx -0.44$ for **1a**BPh₄⁻ (Figure 2). The relative magnitudes of the “ordinary anion” effects and the “BPh₄⁻ effect” in **1b**X⁻ are therefore similar to those in the parent compounds **1a**X⁻.

Correlation with $\Delta G_{\text{t}}^{\circ}$ (H₂O → CH₃CN) of the anions X⁻:

Figures 1 and 2 show that the deshielding of the C(α)-H protons in the **2a**X⁻ and **1a**, **b**X⁻ ion pairs increases in the order SbF₆⁻ < BF₄⁻ < Br⁻ < Cl⁻. An anion's ability to act as hydrogen bond acceptor is related to its single free ion energy of transfer $\Delta G_{\text{t}}^{\circ}$ (H₂O → CH₃CN),^[30] since a large contribution to the transfer energy is the loss of the HO-H...X⁻ hydrogen bonds to the good hydrogen-bond donor H₂O. Figure 3 illustrates that the chemical shifts δ_{H} for the

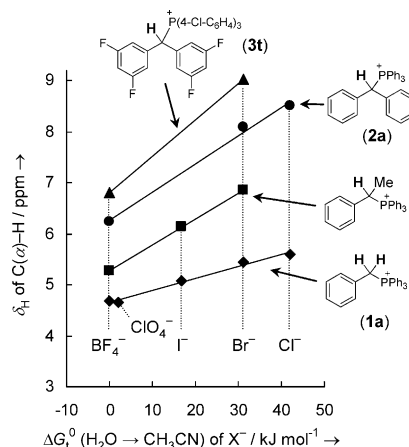


Figure 3. Plot of the ¹H NMR chemical shifts δ_{H} for the C(α)-H in arylmethyl triarylmethyl phosphonium salts (ion pairs) with different counter-anions X⁻ in CD₂Cl₂ (**2a**, **3t**) and CDCl₃ (other salts) against the single free ion energies of transfer $\Delta G_{\text{t}}^{\circ}$ (H₂O → CH₃CN) of the anions X⁻. The points for **1a**BPh₄⁻ and **2a**BPh₄⁻ deviate from the correlation (not shown). See Table S3 in the Supporting Information for numeric values and references.

C(α)-H protons of **2a**X⁻ and other arylmethyl phosphonium salts in CD₂Cl₂ or CDCl₃ correlate linearly with $\Delta G_{\text{t}}^{\circ}$ (H₂O → CH₃CN) of the anions.

Other NMR signals of the phosphonium ions in CD₂Cl₂ solution

Besides the large change in δ_{H} for the C(α)-H protons, Tables 1 and 3 also show the effect of the counter-anion X⁻ on other ³¹P NMR, ¹H NMR, and ¹³C NMR signals of **2a** and **1a** in CD₂Cl₂.

Benzhydryl triphenylphosphonium salts (2aX⁻): The excellent agreement between the ¹H NMR chemical shifts of 2.13×10^{-5} M **2a**SbF₆⁻ and the concentration-independent ¹H NMR chemical shifts of **2a**BPh₄⁻ (Table 1) corroborates the assumption that **2a** SbF₆⁻ mostly exists in the form of the free ions at this concentration. Pairing with the Cl⁻ anion polarizes the bond between α -C and α -H ($\Delta\delta_{\text{H}} = +2.53$ ppm, $\Delta\delta_{\text{C}} = -6.0$ ppm), while the effect on the phosphorus atom is rather small ($\Delta\delta_{\text{P}} = +0.6$ ppm). The coupling constant ¹J_{H,C} = 128.7 Hz for C(α)-H of **2a** BPh₄⁻ is typical for sp³ carbons,^[31] and increases slightly in the presence of the hydrogen-bond acceptor Cl⁻ ($\Delta^1 J_{\text{H,C}} = +2.6$ Hz). A slight increase of ¹J_{H,C} by a few Hz was previously observed for other C-H...X hydrogen bonds and may result from the additional electric field component along the C-H bond in the presence of the hydrogen-bond acceptor.^[32] The ¹J and ²J coupling constants between C(α)-H and P change by $\Delta^1 J_{\text{C,P}} = -2.5$ and $\Delta^2 J_{\text{H,P}} = +1.2$ Hz, respectively.

The *ortho*-protons of the phenyl groups are also deshielded substantially ($\Delta\delta_{\text{H}} \approx +0.50$ ppm), especially if one considers that the effect of the Cl⁻ anion is averaged over six *o*-PPh₃ or four *o*-CHPh₂ protons. Other effects are small: The *iso*- and *ortho*-carbons are also deshielded slightly ($\Delta\delta_{\text{C}} \approx$

Table 3. ^{31}P NMR (162 MHz), ^1H NMR (400 MHz), and ^{13}C NMR (100 MHz) data for the phosphonium ion **1a** in CD_2Cl_2 . Data for **1a** X^- were determined at concentrations where the phosphonium salts exist as ion pairs.

Salt	P^+ δ_{P} [ppm]	CH_2P^+ δ_{H} [ppm] ($^2J_{\text{H,P}}$ $^1J_{\text{H,C}}^{[\text{a}]}$ [Hz])	$o\text{-CH}_2\text{Ph}$ δ_{H} [ppm]	$m\text{-CH}_2\text{Ph}$ δ_{H} [ppm]	$p\text{-CH}_2\text{Ph}$ δ_{H} [ppm]	$o\text{-PPh}_3$ δ_{H} [ppm]	$m\text{-PPh}_3$ δ_{H} [ppm]	$p\text{-PPh}_3$ δ_{H} [ppm]	
1a Cl^-	23.1	5.42 (14.7)	134.6	7.07–7.10	7.14–7.18	7.24–7.29	7.70–7.76	7.60–7.66	7.77–7.82
1a BF_4^-	22.2	4.56 (14.1)	134.2	6.91–6.94	7.20–7.25	7.31–7.36	7.48–7.54	7.65–7.71	7.84–7.88
“free” 1a ^[b]	–[c]	4.39 (14.0)	–[c]	6.87–6.89	7.25–7.28	7.38–7.41	7.43–7.46	7.68–7.72	7.89–7.92
“free” 1a ^[d]	–[c]	4.32 (14.0)	–[c]	6.85–6.89 ^[e]	7.26–7.28	7.38–7.44 ^[f]	7.38–7.44 ^[f]	7.68–7.71	7.89–7.92
1a BPh_4^-	21.6	3.94 (13.8)	133.9	6.73–6.76	7.21–7.28 ^[f]	7.34–7.39	7.21–7.28 ^[f]	7.57–7.62	7.79–7.84
$\Delta(\text{Cl}^-)^{[\text{g}]}$	–[c]	+1.03 (+0.7)	–[c]	~ +0.20	~ –0.10	~ –0.13	~ +0.29	~ –0.07	~ –0.10
$\Delta(\text{BPh}_4^-)^{[\text{h}]}$	–[c]	–0.38 (–0.2)	–[c]	~ –0.12	\leq –0.05	~ –0.05	~ –0.16	~ –0.10	~ –0.09

Salt	CH_2P^+ δ_{C} [ppm] ($^1J_{\text{C,P}}$ [Hz])	$i\text{-CH}_2\text{Ph}$ δ_{C} [ppm] ($^2J_{\text{C,P}}$ [Hz])	$o\text{-CH}_2\text{Ph}$ δ_{C} [ppm] ($^3J_{\text{C,P}}$ [Hz])	$m\text{-CH}_2\text{Ph}$ δ_{C} [ppm] ($^4J_{\text{C,P}}$ [Hz])	$p\text{-CH}_2\text{Ph}$ δ_{C} [ppm] ($^5J_{\text{C,P}}$ [Hz])	$i\text{-PPh}_3$ δ_{C} [ppm] ($^1J_{\text{C,P}}$ [Hz])	$o\text{-PPh}_3$ δ_{C} [ppm] ($^2J_{\text{C,P}}$ [Hz])	$m\text{-PPh}_3$ δ_{C} [ppm] ($^3J_{\text{C,P}}$ [Hz])	$p\text{-PPh}_3$ δ_{C} [ppm] ($^4J_{\text{C,P}}$ [Hz])
1a Cl^-	31.2 (46.9)	128.1 (8.5)	131.9 (5.6)	129.4 (3.3)	129.0 (3.9)	118.5 (85.8)	135.0 (9.8)	130.6 (12.6)	135.5 (3.0)
1a BF_4^-	31.5 (49.0)	127.0 (8.5)	131.5 (5.5)	129.8 (3.2)	129.6 (3.8)	117.6 (86.1)	134.6 (9.7)	130.9 (12.6)	136.1 (3.1)
1a BPh_4^-	31.7 (49.0)	126.5 (8.4)	131.4 (5.4)	129.8 (3.2)	129.7 (3.8)	117.1 (86.4)	134.4 (9.7)	131.0 (12.6)	136.2 (3.0)
$\Delta(\text{total})^{[\text{i}]}$	–0.5 (–2.1)	+1.6 (–0.1)	+0.5 (+0.2)	–0.4 (–0.1)	–0.7 (+0.1)	+1.4 (–0.6)	+0.6 (+0.1)	–0.4 (\pm 0)	–0.7 (\pm 0)

[a] $^1J_{\text{H,C}}$ determined from ^{13}C satellites in the ^1H NMR (600 MHz) spectra. [b] Determined from ^1H NMR (600 MHz) spectrum of a $2.08 \times 10^{-5}\text{M}$ solution of **1a** BF_4^- in CD_2Cl_2 . [c] Not available. [d] Determined from ^1H NMR (600 MHz) spectrum of a $1.75 \times 10^{-5}\text{M}$ solution of **1a** BPh_4^- in CD_2Cl_2 . [e] Superimposed with p -protons of BPh_4^- . [f] Two signals superimposed. [g] “Ordinary anion effect”: Difference between **1a** Cl^- ion pairs and free ions ($2.08 \times 10^{-5}\text{M}$ **1a** BF_4^-). [h] “ BPh_4^- effect”: Difference between **1a** BPh_4^- ion pairs and free ions ($1.75 \times 10^{-5}\text{M}$ **1a** BPh_4^-). [i] Difference between **1a** Cl^- and **1a** BPh_4^- .

+0.5 to +2 ppm) in the presence of Cl^- , while the *meta*- and *para*-positions of the aromatic rings are slightly shielded ($\Delta\delta_{\text{H}} \approx 0$ to -0.18 ppm, $\Delta\delta_{\text{C}} \approx -0.7$ to -1.3 ppm). The effects of Br^- , BF_4^- , and SbF_6^- on the NMR signals of **2a** are similar but less pronounced.

Benzyl triphenylphosphonium salts (1a** X^-):** Table 3 includes two sets of ^1H NMR data for the free $\text{PhCH}_2\text{-PPh}_3^+$ ion (**1a**), one determined from a $2.08 \times 10^{-5}\text{M}$ solution of **1a** BF_4^- , the other from a $1.75 \times 10^{-5}\text{M}$ solution of **1a** BPh_4^- . Again, the good agreement between the two data sets confirms the assignment to the unpaired phosphonium ion **1a**.

Ion-pairing affects the ^1H NMR signals of **1a** Cl^- in a similar way as those of the corresponding benzhydryl triphenylphosphonium ions (**2a**): The $\text{C}(\alpha)\text{-H}$ protons experience the largest deshielding ($\Delta\delta_{\text{H}} \approx +1.03$ ppm, $\Delta^2J_{\text{H,P}} \approx +0.7$ ppm); a smaller but still significant deshielding effect is observed for the *ortho*-protons of the PPh_3 group ($\Delta\delta_{\text{H}} \approx +0.29$ ppm) and the *o*-protons of the benzyl group ($\Delta\delta_{\text{H}} \approx +0.20$ ppm). The *meta*- and *para*-protons of PPh_3 and benzyl are slightly shielded ($\Delta\delta_{\text{H}} \approx -0.07$ to -0.13 ppm).

The same protons which experience a deshielding by pairing with Cl^- are shielded in the **1a** BPh_4^- ion pairs (Table 3): $\Delta\delta_{\text{H}} \approx -0.38$ ppm for $\text{C}(\alpha)\text{-H}$, $\Delta\delta_{\text{H}} \approx -0.16$ and ≈ -0.12 ppm for the *ortho*-protons of the PPh_3 and benzyl groups, respectively. The changes in the chemical shifts of the other protons are in the same direction and of the same magnitude ($\Delta\delta_{\text{H}} \approx -0.08$ to -0.11 ppm) as in **1a** Cl^- .

The ^{31}P NMR signals ($\Delta\delta_{\text{P}} \approx +1.5$ ppm when going from **1a** BPh_4^- to **1a** Cl^-) and the ^{13}C NMR signals of **1a**, including those of $\text{C}(\alpha)$, vary only little with the counteranion X^- (Table 3).

NMR Signals of the anions X^- in CD_2Cl_2 solution

Figure 4a shows the ^{19}F NMR (376 MHz) spectrum of **2a** BF_4^- in CD_2Cl_2 at a concentration where the salt exists as ion pairs ($6 \times 10^{-2}\text{M}$). We observed a 1:1:1:1 quartet ($^1J_{\text{F,B}} \approx 1.2$ Hz) at $\delta_{\text{F}} = -152.0$ ppm for the main isotopomer, $^{11}\text{BF}_4^-$ ($I = 3/2$ for the ^{11}B nucleus), together with the unresolved signal for the ^{10}B ($I = 3$) isotopomer about 0.05 ppm further downfield. The corresponding signal of the boron atom in the ^{11}B NMR (128 MHz) spectrum is at $\delta_{\text{B}} = -2.0$ ppm.

The ^{19}F NMR is sensitive enough so that we could also determine the fluorine chemical shift of the BF_4^- anion at a concentration of $2 \times 10^{-5}\text{M}$, where **2a** BF_4^- exists as free ions in CD_2Cl_2 (Figure 4b). Under these conditions, the signal for the main isotopomer is found at $\delta_{\text{F}} \approx -153.4$ ppm, which is upfield by $\Delta\delta_{\text{F}} \approx -1.4$ ppm compared to the paired **2a** BF_4^- salt.

Figure 4c and d show the heteronuclear NMR spectra of a ca. $6 \times 10^{-2}\text{M}$ solution of **2a** SbF_6^- in CD_2Cl_2 . The antimony isotopes ^{121}Sb ($I = 5/2$) and ^{123}Sb ($I = 7/2$) have similar natural abundances and comparable magnetogyric ratios ($\gamma = 6.4435 \times 10^7$ and 3.4892×10^7 rad $\text{T}^{-1}\text{s}^{-1}$, respectively).^[33] The ^{19}F NMR spectrum of **2a** SbF_6^- in CD_2Cl_2 (Figure 4c) thus features two superimposed signals at $\delta_{\text{F}} = -123.6$ ppm: a sextet with $^1J_{\text{F,Sb}} \approx 1950$ Hz for $^{121}\text{SbF}_6^-$ and an octet with $^1J_{\text{F,Sb}} \approx 1020$ Hz for $^{123}\text{SbF}_6^-$. The ratio of the $^1J_{\text{F,Sb}}$ coupling constants of the two isotopomers corresponds to the ratio of the magnetogyric ratios of the antimony isotopes (i.e., the reduced coupling constants, which are proportional to $^1J_{\text{F,Sb}}/\gamma_{\text{Sb}}$, are the same for both isotopomers). The coupling constant of $^1J_{\text{Sb,F}} \approx 1960$ Hz is also found in the ^{121}Sb NMR (65 MHz) spectrum, in which five lines of the septet at $\delta_{\text{Sb}} \approx 86.2$ ppm are observed (Figure 4d). Due to the broadness of the signal, we could not detect the ^{19}F NMR signal of

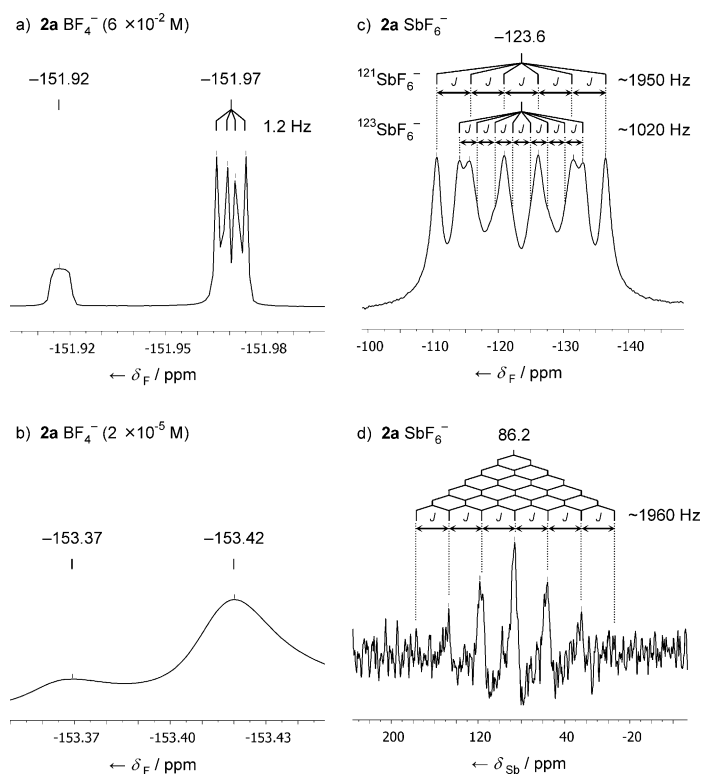


Figure 4. Left: ^{19}F NMR spectra (376 MHz) of $2\mathbf{a}$ BF_4^- in CD_2Cl_2 at concentrations of a) 6×10^{-2} M, or b) 2×10^{-5} M. Right: c) ^{19}F NMR spectrum (376 MHz) and d) ^{121}Sb NMR spectrum (65 MHz) of $2\mathbf{a}$ SbF_6^- in CD_2Cl_2 (ca. 0.06 M).

$2\mathbf{a}\text{SbF}_6^-$ at lower concentrations, where the salt is mostly unpaired.

The NMR data for the BF_4^- and SbF_6^- anions shown in Figure 4a,c,d indicate a very high symmetry of the anions despite the fact that these spectra were recorded under conditions where the phosphonium salts predominantly exist as ion pairs. This indicates that all fluorine atoms are equivalent on the NMR time scale. The interaction between the BF_4^- anion and the phosphonium ion $2\mathbf{a}$ can only be noticed by the slight downfield shift of the signal by $\Delta\delta_{\text{F}} \approx -1.4$ ppm, which indicates the averaged effect over four fluorine atoms.

We also had a closer look at the NMR data of the BPh_4^- anions in concentrated solutions of $1\mathbf{a}, \mathbf{b}\text{BPh}_4^-$ in CD_2Cl_2 . However, the ^{11}B , ^1H , and ^{13}C NMR signals of the BPh_4^- anion in the phosphonium salts $1\mathbf{a}, \mathbf{b}\text{BPh}_4^-$ in CD_2Cl_2 do not differ significantly from those of the free BPh_4^- ions or those of $2\mathbf{a}\text{BPh}_4^-$ which does not show any “ BPh_4^- effect” (Table S4 in the Supporting Information).

Dissociation constants of the phosphonium salts in CD_2Cl_2

The large differences between the $\text{C}(\alpha)\text{-H}$ proton chemical shifts of the unpaired phosphonium ions (e.g., $\delta_{\text{H,unpaired}} = 5.77$ ppm for $2\mathbf{a}$) and the paired phosphonium ions ($\delta_{\text{H,paired}} = \text{maximum } \delta_{\text{H}}$ for the α proton measured at the highest concentration of the salts; see Tables 2, S1, and S2)

allow us to derive the mole fractions of the paired phosphonium ions, $x_{\text{paired,exptl}}$ [Eq. (1)].

$$x_{\text{paired,exptl}} = \frac{\delta_{\text{H}} - \delta_{\text{H,unpaired}}}{\delta_{\text{H,paired}} - \delta_{\text{H,unpaired}}} \quad (1)$$

At phosphonium salt concentrations where $x_{\text{paired,exptl}} \approx 0.5$, we estimated the dissociation constants K_{D} (M) for $1\mathbf{a}, \mathbf{b}\text{X}^-$ and $2\mathbf{a}\text{X}^-$ in CD_2Cl_2 as defined by Equation (2) in which $[\text{R}_4\text{P}^+\text{X}^-]_0$ is the total salt concentration. The resulting values are listed in Table 4.

$$K_{\text{D}} = \frac{[\text{R}_4\text{P}^+]_{\text{unpaired}} \cdot [\text{X}^-]_{\text{unpaired}}}{[\text{R}_4\text{P}^+\text{X}^-]_{\text{paired}}} = \frac{(1 - x_{\text{paired,exptl}})^2}{x_{\text{paired,exptl}}} \cdot [\text{R}_4\text{P}^+\text{X}^-]_0 \quad (2)$$

Table 4. Dissociation constants K_{D} [M] for phosphonium salts $1\mathbf{a}, \mathbf{b}\text{X}^-$ and $2\mathbf{a}\text{X}^-$ with different counter-anions X^- in CD_2Cl_2 .

X^-	$\Delta G_{\text{acid}}^{\text{[a]}}$ [kcal mol $^{-1}$]	$\Delta G_{\text{t}}^{\text{[b]}}$ [kJ mol $^{-1}$]	$K_{\text{D}}^{\text{[c]}}$ [M]		
			$1\mathbf{a}\text{X}^-$	$1\mathbf{b}\text{X}^-$	$2\mathbf{a}\text{X}^-$
BPh_4^-	— ^[d]	−32.8	2.5×10^{-4}	1.1×10^{-4}	^[e]
SbF_6^-	256	— ^[d]	^[f]	^[f]	6×10^{-4}
BF_4^-	288	(−0) ^[g]	(1×10^{-4})	(5×10^{-5})	2.2×10^{-4}
Br^-	315	31.3	^[f]	2.9×10^{-5}	7.6×10^{-5}
Cl^-	324	42.1	6.8×10^{-5}	^[f]	3.4×10^{-5}
$\text{p}K_{\text{a}}$ for $\text{C}(\alpha)\text{-H}$ in DMSO:			17.6 ^[h]	14.6 ^[h]	(−9) ^[i]

[a] Calculated ΔG_{acid} (298 K) for deprotonation of the conjugate acids HX in the gas phase.^[34] [b] Single free ion energies of transfer ΔG_{t}^0 ($\text{H}_2\text{O} \rightarrow \text{CH}_3\text{CN}$, 25 °C) for the anions X^- .^[30] [c] Dissociation constants in CD_2Cl_2 based on δ_{H} of the $\text{C}(\alpha)\text{-H}$ protons; this work. [d] Not available. [e] No effect of X^- on δ_{H} of the $\text{C}(\alpha)\text{-H}$ protons. [f] Not determined. [g] For BF_4^- , $\Delta G_{\text{t}}^0 \approx 0$ was estimated.^[35] [h] From ref. [6]. [i] Estimated from the correlation equation published in ref. [5] and $\text{p}K_{\text{a}}$ 30.6 for Ph_2CH_2 .^[29]

With this method, more reliable values of K_{D} can be obtained than by evaluating K_{D} from all investigated solutions, which also include those in which paired or non-paired species are highly dominating. The mole fractions of unpaired ions $x_{\text{paired,calcd}}$ calculated from these K_{D} values are in fair agreement with the experimental values $x_{\text{paired,exptl}}$ (Tables 2, S1, S2). The K_{D} values for $1\mathbf{a}, \mathbf{b}\text{BF}_4^-$ are only rough estimates, as the effect of ion pairing on δ_{H} is small for these salts ($\Delta\delta_{\text{H}} \approx 0.17$ to 0.23 ppm for $\text{C}(\alpha)\text{-H}$ protons) and we cannot determine $\delta_{\text{H,unpaired}}$ for the unpaired ions $1\mathbf{a}, \mathbf{b}$ very accurately.

The dissociation constants K_{D} determined in this manner decrease in the order $\text{SbF}_6^- > \text{BF}_4^- > \text{Br}^- > \text{Cl}^-$ (Table 4). Thus, the degree of association of the phosphonium salts increases with the deshielding of the $\text{C}(\alpha)\text{-H}$ protons in the respective ion pairs ($\text{SbF}_6^- < \text{BF}_4^- < \text{Br}^- < \text{Cl}^-$). In agreement with the higher $\text{C}(\alpha)\text{-H}$ acidity of $1\mathbf{b}$ compared with $1\mathbf{a}$,^[6] the dissociation constants K_{D} for all $1\mathbf{b}\text{X}^-$ salts are smaller than those for the corresponding $1\mathbf{a}\text{X}^-$ salts (e.g., K_{D} of $1\mathbf{b}\text{Br}^-$ is already smaller than that of $1\mathbf{a}\text{Cl}^-$ although

Cl^- is more basic than Br^- (Table 4). Since **2a** has an even higher $\text{C}(\alpha)\text{-H}$ acidity than **1b**, one might also expect lower dissociation constants K_D for **2aX**⁻ than for **1bX**⁻. On the contrary, the K_D values for **2aX**⁻ are higher than for **1bX**⁻ (Table 4), that is, the salts **2aX**⁻ dissociate more readily. The reason for this may be a combination of steric hindrance and a statistical effect due to the fact that there is only one $\text{C}(\alpha)\text{-H}$ proton in the benzhydryl derivatives **2aX**⁻ but two in the benzyl derivatives **1bX**⁻.

It should be noted, however, that the differences in K_D are rather small, and all K_D values are in the same order of magnitude as previously reported for benzhydrylium, tritylium, pyrylium, and tetraalkylammonium salts in CH_2Cl_2 .^[36]

Effect of the solvent: ¹H NMR Signals for α protons of **2a** in CD_3CN solution

In CD_3CN , variation of the counteranion X^- has a much smaller effect on the ¹H NMR chemical shifts of $\text{C}(\alpha)\text{-H}$ of **2aX**⁻ than in CD_2Cl_2 . As in CD_2Cl_2 , the δ_{H} values for **2aBPh**₄⁻ do not vary with the concentration ($\delta_{\text{H}} = 6.27$ ppm, Figure 5). The very similar δ_{H} for **2aBF**₄⁻ and **2aSbF**₆⁻ suggest that these compounds are also mostly unpaired at concentrations of $\sim 1 \times 10^{-2}$ M in CD_3CN .

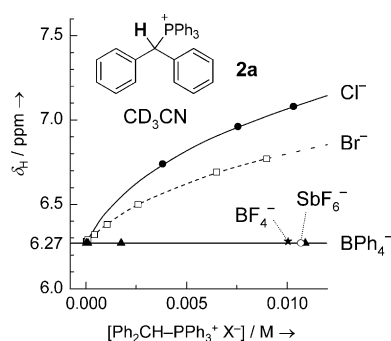


Figure 5. Concentration-dependent ¹H NMR (600 MHz, 27 °C) chemical shifts δ_{H} of the benzylic $\text{C}(\alpha)\text{-H}$ protons of **2aX**⁻ with different counteranions $\text{X}^- = \text{Cl}^-$ (●), Br^- (□), BF_4^- (★), SbF_6^- (○), or BPh_4^- (▲) in CD_3CN .

The chemical shifts of $\delta_{\text{H}} \leq 6.29$ ppm determined for the $\text{C}(\alpha)\text{-H}$ protons of **2aBr**⁻ in CD_3CN at concentrations $\leq 1 \times 10^{-4}$ M indicate that ion pairing is negligible in this concentration range (Table S5 in the Supporting Information). At larger concentrations, the phosphonium halides do form ion pairs to some extent. However, the δ_{H} values of the phosphonium halides in CD_3CN do not reach a plateau in the concentration range where **2aBr**⁻ is soluble in CD_3CN ($< 1 \times 10^{-2}$ M). Therefore, we cannot estimate the degree of ion pairing or the dissociation constants K_D in CD_3CN from the NMR data.

Effect of $\text{C}(\alpha)\text{-H}$ acidity: Substituent effects on the NMR spectra of phosphonium salts

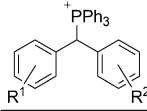
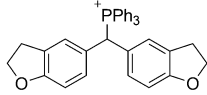
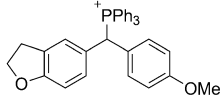
In a series of benzhydryl triphenylphosphonium salts $\text{Ar}_2\text{CH-PPh}_3^+ \text{X}^-$ (**2X**⁻) with different Ar groups, the acidities of the $\text{C}(\alpha)\text{-H}$ groups increase with the electron-withdrawing character of the substituents on the benzhydryl moiety. The series of substituted benzhydryl triphenylphosphonium tetrafluoroborates **2a-tBF**₄⁻ (Table 5), which we required for our laser flash photolysis experiments,^[19] can thus be employed to study the interaction between $\text{C}(\alpha)\text{-H}$ and BF_4^- as a function of $\text{C}(\alpha)\text{-H}$ acidity.

The NMR data for the **2a-tBF**₄⁻ ion pairs in CD_2Cl_2 solution are collected in Table 5, where the salts **2a-tBF**₄⁻ are arranged according to the sums of their substituents' σ^- parameters.^[37] We use the σ^- parameters as a measure for the $\text{C}(\alpha)\text{-H}$ acidities of the phosphonium ions here, because the $\text{p}K_{\text{a}}$ values of **2a-tBF**₄⁻ are not available and the $\text{p}K_{\text{a}}$ values of the closely related benzyl triphenylphosphonium salts in DMSO have been shown to correlate with the σ^- parameters of the benzyl substituents.^[6] The ¹H NMR chemical shifts of the $\text{C}(\alpha)\text{-H}$ protons increase from $\delta_{\text{H}} \approx 6.04$ to ≈ 6.80 ppm when the substituents of the benzhydryl group are varied from electron-donating (**2b**) to strongly electron-withdrawing (**2s** or **2t**). Figure S1 in the Supporting Information displays a moderate correlation of δ_{H} for the $\text{C}(\alpha)\text{-H}$ protons of **2BF**₄⁻ with the sums of the σ^- parameters.

If the observed increase of δ_{H} of the $\text{C}(\alpha)\text{-H}$ protons and the less pronounced concomitant variations in δ_{C} of the $\text{C}(\alpha)$ atom and δ_{P} of the phosphorus atom (Table 5) are linked with stronger interactions with the BF_4^- anion, one should also observe the effect in the ¹⁹F NMR spectra of the BF_4^- ions. Indeed, the ¹⁹F NMR chemical shifts for ¹¹ BF_4^- increase from $\delta_{\text{F}} \approx -152.2$ to ≈ -150.4 ppm when going from **2bBF**₄⁻ to **2tBF**₄⁻ (Figure 6 and Table 5). Thus, the greater the $\text{C}(\alpha)\text{-H}$ acidity of the phosphonium ion **2**, the larger the upfield shift $\Delta\delta_{\text{F}}$ for the BF_4^- anion due to the increasing strength of ion pairing with the phosphonium ion. The increasing $\text{C}(\alpha)\text{-H}$ acidity from **2aBF**₄⁻ ion pairs to **2tBF**₄⁻ ion pairs causes approximately the same shifts in the ¹H and ¹⁹F NMR signals ($\Delta\delta_{\text{H}} \approx +0.45$ ppm and $\Delta\delta_{\text{F}} \approx +1.6$ ppm) as going from the free ions **2a** and BF_4^- to the **2aBF**₄⁻ ion pairs ($\Delta\delta_{\text{H}} \approx +0.46$ ppm and $\Delta\delta_{\text{F}} \approx +1.4$ ppm) (Figure 6). In analogous series of neutral benzhydryl derivatives such as benzhydryl halides, substituent variations induce considerably smaller changes of δ_{H} for the $\text{C}(\alpha)\text{-H}$ protons in the other direction (see Figure S1 in the Supporting Information).

Moreover, the α protons of the unpaired benzyl triphenylphosphonium ions $\text{PhCH}_2\text{-PPh}_3^+$ (**1a**) and $p\text{-(CF}_3\text{)}_2\text{-C}_6\text{H}_4\text{-CH}_2\text{-PPh}_3^+$ (**1b**) have very similar δ_{H} values despite the differing substitution patterns (see Tables S1 and S2 in the Supporting Information). All these observations suggest that the variations in δ_{H} of the benzhydryl methine protons observed for the ion pairs of the differently substituted benzhydryl triphenylphosphonium tetrafluoroborates **2BF**₄⁻

Table 5. Selected NMR data for triphenylphosphonium tetrafluoroborates **2a–t**BF₄[−] in CD₂Cl₂ solution under conditions where the phosphonium salts exist as ion pairs.

Salt			Σσ ^{−[a]}	P ⁺ –C(α)–H			¹¹ BF ₄ ^{−[b]}
	R ¹	R ²		δ _H [ppm] (² J _{H,P} [Hz])	δ _C [ppm] (¹ J _{C,P} [Hz])	δ _P [ppm]	
<i>ion pairs</i>							
2b BF ₄ [−]			−[c]	6.04 (17.2)	49.1 (42.8)	20.5	−152.2 (−[d])
2c BF ₄ [−]			−[c]	6.04 (17.2)	48.9 (43.1)	20.6	−152.3 (−[d])
2d BF ₄ [−]	<i>p</i> -OMe	<i>p</i> -OMe	−0.52	6.15 (17.3)	48.2 (43.2)	20.8	−152.1 (−[d])
2e BF ₄ [−]	<i>p</i> -OMe	<i>p</i> -Me	−0.43	6.08 (17.2)	48.9 (43.5)	21.0	−152.4 (1.0)
2f BF ₄ [−]	<i>p</i> -OMe	<i>p</i> -OPh	−0.36	6.18 (17.4)	48.4 (43.5)	21.0	−152.1 (1.1)
2g BF ₄ [−]	<i>p</i> -Me	<i>p</i> -Me	−0.34	6.04 (17.2)	49.4 (43.6)	21.1	−152.3 (1.1)
2h BF ₄ [−]	<i>p</i> -OMe	H	−0.26	6.20 (17.2)	48.9 (43.5)	21.3	−152.1 (1.1)
2i BF ₄ [−]	<i>p</i> -Me	H	−0.17	6.20 (17.4)	49.1 (43.8)	21.5	−152.2 (1.1)
2j BF ₄ [−]	<i>p</i> -OPh	H	−0.10	6.31 (17.4)	48.6 (43.8)	21.5	−151.8 (1.1)
2k BF ₄ [−]	<i>p</i> -F	<i>p</i> -F	−0.06	6.49 (17.7)	47.3 (44.7)	21.9	−151.3 (−[d])
2l BF ₄ [−]	<i>p</i> -F	H	−0.03	6.40 (17.5)	48.1 (44.3)	21.9	−151.5 (1.2)
2a BF ₄ [−]	H	H	0.00	6.23 (17.4)	49.6 (43.9)	21.8	−152.0 (1.2)
2m BF ₄ [−]	<i>m</i> -F	H	0.34	6.39 (17.5)	48.5 (44.5)	22.0	−151.6 (1.1)
2n BF ₄ [−]	<i>p</i> -Cl	<i>p</i> -Cl	0.38	6.48 (17.7)	47.4 (44.6)	21.8	−151.2 (1.2)
2o BF ₄ [−]	<i>p</i> -CF ₃	H	0.65	6.53 (17.7)	48.4 (44.7)	22.1–22.2	−151.4 (1.2)
2p BF ₄ [−]	<i>m,m'</i> -F ₂	H	0.68	6.51 (17.5)	47.9 (45.1)	22.2	−151.4 (1.2)
2q BF ₄ [−]	<i>m</i> -F	<i>m</i> -F	0.68	6.52 (17.6)	47.7 (45.0)	22.3	−151.1 (1.2)
2r BF ₄ [−]	<i>m,m'</i> -F ₂	<i>m</i> -F	1.02	6.61 (17.6)	47.1 (45.6)	22.5	−150.8 (1.3)
2s BF ₄ [−]	<i>p</i> -CF ₃	<i>p</i> -CF ₃	1.30	6.80 (17.8)	47.5 (45.3)	22.4–22.5	−150.7 (−[d])
2t BF ₄ [−]	<i>m,m'</i> -F ₂	<i>m,m'</i> -F ₂	1.36	6.68 (17.6)	46.6 (46.2)	22.6	−150.4 (1.3)
<i>“free” ions</i>							
2a ^[e,g]	H	H	0.00	5.77 (17.0)	−[c]	−[c]	−
BF ₄ ^{−[f,g]}	−	−	−	−	−	−	−153.4 (−[d])

[a] From ref. [37]. [b] Isotopomer signal for ¹⁰BF₄[−] downfield by Δδ_F < +0.1 ppm. [c] Not available. [d] Not resolved. [e] Determined from ¹H NMR (600 MHz) spectrum of a 2.13 × 10^{−5} M solution of **2a** SbF₆[−] in CD₂Cl₂. [f] Determined from ¹⁹F NMR (376 MHz) spectrum of a ~2 × 10^{−5} M solution of **2a** BF₄[−] in CD₂Cl₂. [g] At the employed concentrations, the salts predominantly exist in the form of the free (unpaired) ions.

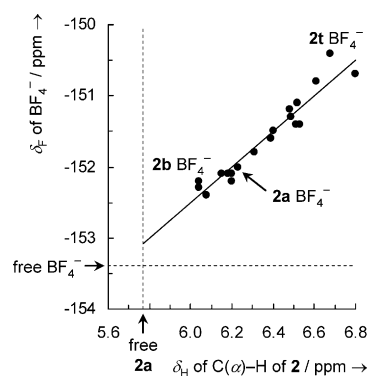


Figure 6. Correlation of ¹⁹F NMR (376 MHz) chemical shifts δ_F of the BF₄[−] anions versus the ¹H NMR (400 MHz) chemical shifts δ_H of the C(α)–H protons of the phosphonium ions **2** in the ion pairs **2a–t**BF₄[−] in CD₂Cl₂ (δ_F = 2.51δ_H − 167.54; R² = 0.9299). The dashed lines show the chemical shifts of the free ions **2a** and BF₄[−].

mainly result from the different interactions of the methine protons with the BF₄[−] anions.

The C(α)–H acidities of the benzhydryl triarylphosphonium ions Ar₂CH–PAR₃⁺X[−] are also affected by variation of the PAR₃ moiety. Table S6 in the Supporting Information illustrates that the δ_H values for the C(α)–H protons for the tris(4-chlorophenyl)phosphonium salts Ar₂CH–P(*p*-Cl-C₆H₄)₃⁺BF₄[−] (**3BF**₄[−]) are 0.15 to 0.48 ppm higher and the δ_F values for the BF₄[−] anion are 0.7 to 2.1 ppm higher than for the corresponding triphenylphosphonium salts Ar₂CH–PPh₃⁺BF₄[−] (**2BF**₄[−]). Thus, electron-withdrawing substituents in the triphenylphosphonium group have analogous effects on δ_H and δ_F as substituents in the benzhydryl group.

Calculations and X-ray Analyses

To learn more about the structure of the phosphonium salt ion pairs in solution, we will now compare the NMR data with the results of quantum chemical calculations as well as with the C–H⋯X[−] interactions in the crystals. The structural

features in solution and in the crystals resemble each other and will therefore be discussed together for each compound.

Strong hydrogen bonds are characterized by short H \cdots X $^-$ distances and C–H \cdots X $^-$ angles close to 180°, but there are no clear cut-off criteria to decide whether a C–H \cdots X $^-$ contact should be considered as a hydrogen bond. According to the latest IUPAC definition of the hydrogen bond,^[8] weak hydrogen bonds may also be longer than the sum of the van der Waals radii, and the angle of a hydrogen bond “should preferably be above 110°”. In the calculated solution structures, as well as in the crystal structures, we have considered all H \cdots X $^-$ distances up to 2.90 Å, and also added some notable longer contacts, the most important of which are shown as dashed lines in the Figures. Particularly short (shorter than the sum of the van der Waals radii)^[38] or close to linear contacts (C–H \cdots X $^-$ angle \geq 160°) are indicated by bold type in the Tables listing the lengths and angles of the C–H \cdots X $^-$ contacts.

Benzhydryl triphenylphosphonium salts (2aX $^-$)

Calculated structures in CH₂Cl₂ solution: The solution-phase structures of the salts 2aX $^-$ in dichloromethane (Figure 7a–d) were determined by DFT calculations on the M06-2X 6-31+G(d,p) level of theory with a polarizable continuum model to describe the effect of the solvent.^[39–43] The solution structure of the BPh₄ $^-$ salt was not calculated due to the large size of the ions. Table 6 lists the distances and angles of the C–H \cdots X $^-$ contacts in the ion pairs.

Crystal structures: Crystal structures of salts of the Ph₂CH–PPh₃ $^+$ cation (2a) have not been described previously. In this work, we have therefore determined the crystal structures of the same salts 2aX $^-$ which we have investigated in solution. Only 2a BPh₄ $^-$ crystallizes as very long thin needles, and we could not obtain single crystals of sufficient size in all three dimensions to determine the structure of this salt by X-ray diffraction. In each of the crystal structures, the phosphonium ions have many C–H \cdots X $^-$ interactions with one particular anion and fewer contacts with other anions (Figure 7e–h). The solid state structures thus resemble the 1:1 ion pairs which are present in solution (Figure 7a–d). Table 7 lists the distances and angles of the closest C–H \cdots X $^-$ contacts in the crystals.

Benzhydryl triphenylphosphonium chloride (2a Cl $^-$): The calculated structure of 2a Cl $^-$ in CH₂Cl₂ (Figure 7a) shows two strong hydrogen bonds between the Cl $^-$ anion and the C(α)–H and one *o*-PPh₃ proton (H19 \cdots Cl distance 2.44 Å and C19–H19 \cdots Cl angle 176°; H2 \cdots Cl distance 2.52 Å and C2–H2 \cdots Cl angle 176°) (Table 6). The positioning of the chloride anion near the C(α)–H and *o*-PPh₃ protons is further stabilized by two weaker hydrogen bonds to *o*-CPh₂ protons of both phenyl rings of the benzhydryl group (H31 \cdots Cl distance 2.81 Å and C31–H31 \cdots Cl angle 147°; H25 \cdots Cl distance 3.13 Å and C25–H25 \cdots Cl angle 140°).

These interactions seem to be so favorable that they are also found in the crystal (Figure 7e), which shows two short contacts between Cl $^-$ and the C(α)–H as well as one *o*-CPh₂ proton (H19 \cdots Cl distance 2.49 Å and C19–H19 \cdots Cl angle 166°; H31 \cdots Cl distance 2.82 Å, C31–H31 \cdots Cl angle 147°), but a significantly longer distance between the Cl $^-$ anion and the *o*-PPh₃ proton (H2 \cdots Cl distance 3.00 Å and C2–H2 \cdots Cl angle 161°) (Table 7). The packing of the molecules is controlled by additional C–H \cdots Cl $^-$ hydrogen bonds involving some of the *meta*- and *para*-protons of the PPh₃ group, resulting in a different orientation of the phenyl groups compared to the solution structure. Particularly strong is the C–H \cdots Cl $^-$ interaction for one of the *p*-PPh₃ protons (H10 \cdots Cl distance 2.58 Å and C10–H10 \cdots Cl angle 171°). Thus, the distances and angles for the two shortest C–H \cdots Cl $^-$ interactions in crystals of 2a Cl $^-$ come very close to the typical values of O–H \cdots Cl $^-$ hydrogen bonds.^[3]

Benzhydryl triphenylphosphonium bromide (2a Br $^-$): The calculated structure of the 2a Br $^-$ ion pair in CH₂Cl₂ (Figure 7b) closely resembles that of the chloride (Figure 7a); only the distances between the hydrogen (or carbon) atoms and the halide ion are longer by 0.1 to 0.2 Å (Table 6).

Again, a similar motif is found in the 2a Br $^-$ crystal (Figure 7f and Table 7): The strongest interactions between cation and anion are the hydrogen bonds between the Br $^-$ anion and the C(α)–H and *o*-PPh₃ protons (H7 \cdots Br distance 2.90 Å and C7–H7 \cdots Br angle 172°; H6 \cdots Br distance 2.85 Å, C6–H6 \cdots Br angle 167°), as well as the interaction of one *m*-PPh₃ proton with a second bromide anion (H16 \cdots Br distance 2.81 Å and C16–H16 \cdots Br angle 151°). Weaker interactions are observed between Br $^-$ and the *o*-CHPh₂ protons as well as another *o*-PPh₃ proton, but these are already in the same range as the interactions between Br $^-$ and various phenyl protons of further surrounding phosphonium ions (\geq 3.0 Å).

Benzhydryl triphenylphosphonium tetrafluoroborate (2a BF₄ $^-$): In the calculated structure of 2a BF₄ $^-$ in CH₂Cl₂ solution (Figure 7c), the C(α)–H (H19) as well as one *o*-PPh₃ (H12) and one *o*-CPh₂ proton (H31) show bifurcated hydrogen bonds with two of the fluorine atoms (F2 and F3) (Table 6). Additionally, the *o*-PPh₃ proton (H12) has a third C–H \cdots F–BF₃ $^-$ interaction with a third fluorine atom (F1), and the second phenyl group of the benzhydryl moiety also shows one contact between *o*-CPh₂ (H25) and F–BF₃ $^-$ (F3).

In the 2a BF₄ $^-$ crystal, all fluorine atoms of the BF₄ $^-$ anion exhibit multifurcated hydrogen bonds to several surrounding phosphonium ions. The usual pattern of close interactions between the anion and the C(α)–H proton (H19), one *o*-PPh₃ (H12), and one *o*-CPh₂ proton (H31) is also found (Figure 7g and Table 7), but it differs a bit from the calculated structure in solution. Again, the shortest contact is the C(α)–H \cdots F–BF₃ $^-$ interaction (H19 \cdots F2 distance 2.23 Å and C19–H19 \cdots F2 angle 158°), but in the crystal, only the *o*-PPh₃ proton (H12) shows bifurcated hydrogen bonds, while the other interactions are directed towards only one of the fluorine atoms. The fourth close C–H \cdots F–

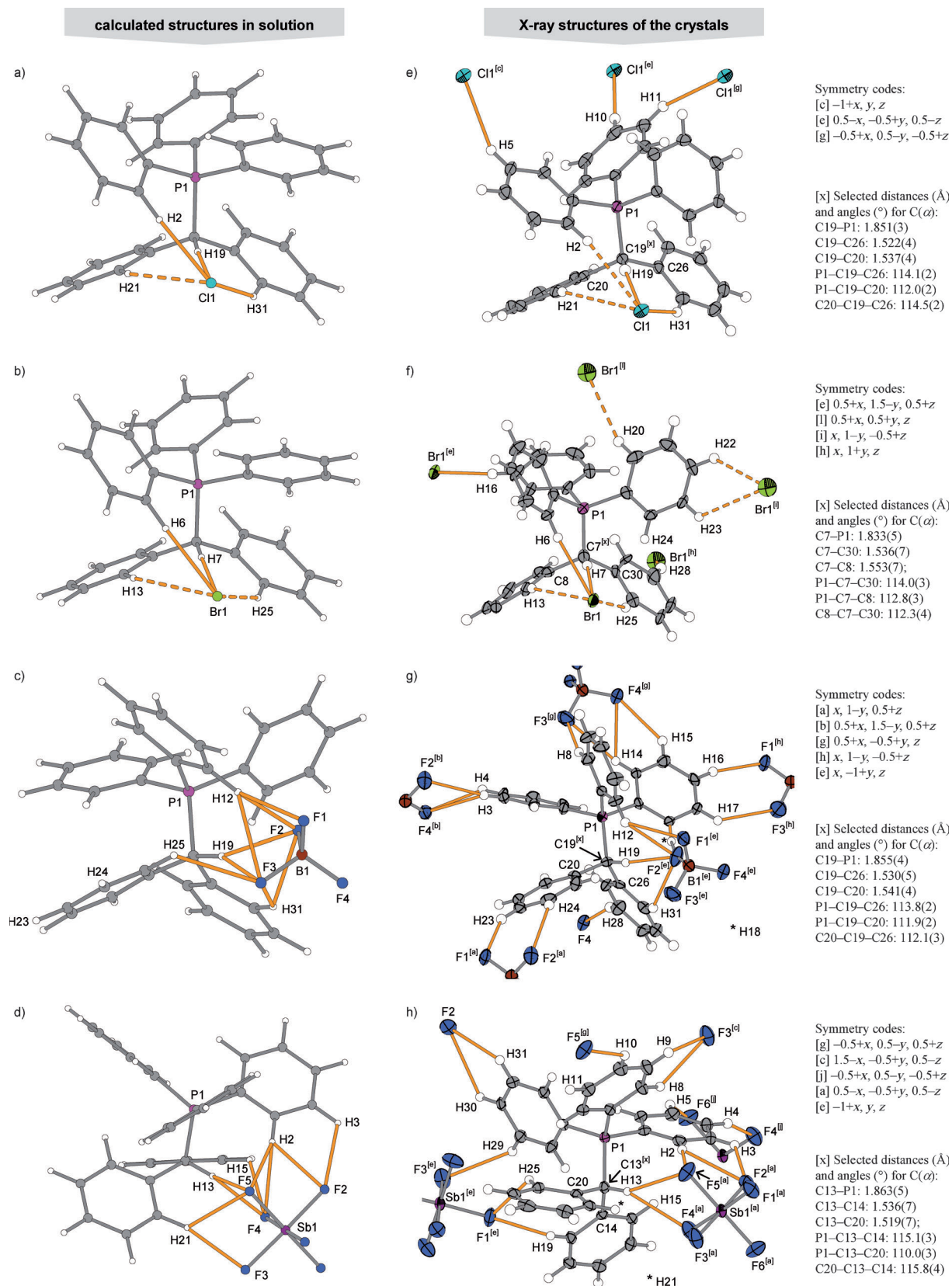


Figure 7. a)–d) Calculated structures of $\text{Ph}_2\text{CH-PPh}_3^+ \text{X}^-$ ($2\mathbf{aX}^-$) ion pairs in CH_2Cl_2 solution: a) $2\mathbf{aCl}^-$, b) $2\mathbf{aBr}^-$, c) $2\mathbf{aBF}_4^-$, d) $2\mathbf{aSbF}_6^-$. The numbering corresponds to the atom numbers in the crystal structures. e)–h) X-ray structures of the salts $\text{Ph}_2\text{CH-PPh}_3^+ \text{X}^-$ ($2\mathbf{aX}^-$): e) $2\mathbf{aCl}^-$, f) $2\mathbf{aBr}^-$, g) $2\mathbf{aBF}_4^-$, h) $2\mathbf{aSbF}_6^-$. All C–H...X contacts with $d(\text{H}\cdots\text{X}) \leq 2.90 \text{ \AA}$ are shown as orange lines, selected longer contacts are indicated by dashed lines. For C–H...X bond lengths and angles, see Tables 6 and 7.

Table 6. Calculated distances and angles of C–H...X[−] contacts in Ph₂CH–PPh₃⁺X[−] (**2a**X[−]) ion pairs in CH₂Cl₂ solution.

Salt	Donor ^[a]	Acceptor ^[a]	d(C–H)	d(H...X [−])	d(C...X [−])	∠(C–H...X [−])
				[Å]	[Å]	[°]
2a Cl [−]	H19 (α-H)	Cl1	1.1022	2.44	3.54	176
	H2	Cl1	1.0907	2.52	3.61	176
	H31	Cl1	1.0881	2.81	3.77	147
	H21	Cl1	1.0869	3.13	4.02	140
2a Br [−]	H7 (α-H)	Br1	1.1021	2.64	3.74	177
	H6	Br1	1.0901	2.68	3.77	178
	H25	Br1	1.0877	2.93	3.92	152
2a BF ₄ [−]	H19 (α-H)	F2	1.0968	2.30	3.24	142
	H19 (α-H)	F3		2.20	3.23	156
	H12	F2	1.0861	2.25	3.29	158
	H12	F1		2.38	3.29	140
	H12	F3		2.66	3.56	140
	H31	F2	1.0863	2.57	3.32	126
	H31	F3		2.71	3.63	142
2a SbF ₆ [−]	H25	F3	1.0857	2.57	3.32	125
	H13 (α-H)	F4	1.0977	2.28	3.28	151
	H13 (α-H)	F5		2.44	3.37	141
	H2	F4	1.0860	2.74	3.45	122
	H2	F5		2.30	3.36	165
	H2	F2		2.42	3.19	126
	H3	F2	1.0848	2.66	3.30	117
H21	F5	1.0865	2.59	3.34	126	
H21	F3		2.44	3.50	165	
H15	F4	1.0852	2.54	3.22	120	

[a] See Figure 7 for numbering of atoms.

BF₃[−] contact is now to a second *o*-PPh₃ proton (H18) instead of the second *o*-CPh₂ proton. This subtle variation between the solution and crystal structures is caused by the additional interactions between BF₄[−] and the other surrounding phosphonium ions in the crystal (Figure 7g and Table 7).

Benzhydryl triphenylphosphonium hexafluoroantimonate (2aSbF₆[−]): According to the calculations, the fluorine atoms of the SbF₆[−] anions in the **2aSbF₆[−]** ion pairs in CH₂Cl₂ solution also form multifurcated hydrogen bonds (Figure 7d and Table 6). The C(α)–H proton forms a short bifurcated hydrogen bond with two of the fluorine atoms (H13...F4 distance 2.28 Å and C13–H13...F4 angle 151°; H13...F5 distance 2.44 Å and C13–H13...F5 angle 141°). The same two fluorine atoms are also involved in a bifurcated hydrogen bond with one of the *o*-PPh₃ protons (H2...F5 distance 2.30 Å and C2–H2...F5 angle 165°; H2...F4 distance 2.74 Å and C2–H2...F4 angle 122°), and each of them also has a weaker interaction with an *o*-CPh₂ proton (H15 or H21) (Table 6). A further strong hydrogen bond is found between one of the *o*-CPh₂ protons and a third fluorine atom (H21...F3 distance 2.44 Å and C21–H21...F3 angle 165°). Two weaker interactions are observed between the *o*-PPh₃ (H2) and *m*-PPh₃ (H3) protons and a fourth fluorine atom (F2) (Table 6).

The fluorine atoms of the SbF₆[−] anions in the **2aSbF₆[−]** crystal also form multifurcated hydrogen bonds (Figure 7h and Table 7), but the C–H...F interactions differ somewhat from those in CH₂Cl₂ solution. The closest C–H...F–SbF₅[−]

Table 7. Distances and angles of C–H...X[−] contacts in crystals of Ph₂CH–PPh₃⁺X[−] (**2a**X[−]).

Salt	Donor ^[a]	Acceptor ^[a]	Code ^[a]	d(H...X [−])	d(C...X [−])	∠(C–H...X [−])	
				[Å]	[Å]	[°]	
2a Cl [−]	H19 (α-H)	Cl1	–	2.49(3)	3.444(3)	166(2)	
	H31	Cl1	–	2.82	3.654(3)	147	
	H2	Cl1	–	3.00	3.913 (3)	161	
	H21	Cl1	–	3.20	3.900(3)	132	
	H10	Cl1	e	2.58	3.526(3)	171	
	H5	Cl1	c	2.76	3.573(3)	144	
	H11	Cl1	g	2.81	3.526(3)	133	
	2a Br [−]	H7 (α-H)	Br1	–	2.90	3.894(5)	172
		H6	Br1	–	2.85	3.781(5)	167
		H13	Br1	–	3.19	4.000(5)	144
		H25	Br1	–	3.14	4.024(5)	156
H24 ^[b]		Br1	–	3.68	4.491(5)	146	
H16		Br1	e	2.81	3.672(6)	151	
H20		Br1	l	3.02	3.915(6)	158	
H22		Br1	i	3.05	3.734(5)	131	
H23		Br1	i	3.22	3.828(5)	123	
H28		Br1	h	3.38	4.267(5)	156	
2a BF ₄ [−]		H19 (α-H)	F2	e	2.23	3.218(4)	158
	H18	F2	e	2.59	3.340(4)	136	
	H12	F2	e	2.53	3.329(4)	141	
	H12	F1	e	2.80	3.450(4)	127	
	H31	F2	e	2.73	3.423(4)	130	
	H23	F1	a	2.44	3.259(4)	144	
	H24	F2	a	2.84	3.643(5)	143	
	H3	F2	b	2.54	3.467(3)	164	
	H3	F4	b	2.67	3.236(4)	119	
	H4	F4	b	2.70	3.247(4)	117	
	H8	F3	g	2.56	3.482(5)	163	
2a SbF ₆ [−]	H14	F3	g	2.59	3.527(4)	170	
	H14	F4	g	2.62	3.192(4)	119	
	H15	F4	g	2.60	3.179(5)	120	
	H16	F1	h	2.29	3.221(3)	167	
	H17	F3	h	2.62	3.357(4)	135	
	H28	F4	–	2.48	3.407(4)	164	
	2a SbF ₆ [−]	H13 (α-H)	F4	a	2.67	3.505(5)	151
		H13 (α-H)	F5	a	2.84	3.683(5)	153
		H2	F5	a	2.42	3.372(6)	178
		H2	F2	a	2.72	3.293(5)	120
		H3	F2	a	2.60	3.234(5)	125
H21 ^[b]		F3	a	3.16	4.096(5)	169	
H25		F1	e	2.85	3.561(6)	133	
H19		F1	e	2.58	3.074(5)	113	
H29		F3	e	2.74	3.208(5)	111	
H31		F2	–	2.59	3.265(5)	129	
H30		F2	–	2.80	3.365(6)	119	
H10	F5	g	2.66	3.373(6)	132		
H11 ^[b]	F5	g	2.95	3.511(6)	119		
H8	F3	c	2.50	3.097(6)	121		
H9	F3	c	2.53	3.114(6)	120		
H4	F4	j	2.54	3.374(6)	147		
H5	F6	j	2.76	3.571(6)	144		

[a] See Figure 7 for numbering of atoms and symmetry codes. [b] These contacts are not shown in Figure 7.

contact is between an *o*-PPh₃ proton and one of the fluorine atoms (H2...F5 distance 2.42 Å and C2–H2...F5 angle 178°). This proton also has a second weaker interaction with another fluorine atom (F2), which also forms a hydrogen bond to the adjacent *m*-PPh₃ proton (H3). The bifurcated hydrogen bonds between the C(α)–H proton and the SbF₆[−] anion are significantly longer than in solution or in the crystals of

the other salts (H13...F4 distance 2.67 Å and C13-H13...F4 angle 151°; H13...F5 distance 2.84 Å and C13-H13...F5 angle 153°), and the typical interaction with one or more *o*-CPh₂ protons is not found (Figure 7 h). Instead, the *o*-CPh₂ protons (H19 and H25) form hydrogen bonds to a second SbF₆⁻ anion which is located on the far side of the C(α)-H proton. The packing of the ions is also influenced by several other contacts between the protons of the PPh₃ groups and neighboring SbF₆⁻ anions (Figure 7 h and Table 7).

Benzyl triphenylphosphonium salts (1X⁻)

Halide and tetrafluoroborate salts: The calculated structures of **1aCl⁻** and **1aBF₄⁻** in CH₂Cl₂ solution closely resemble those of the benzhydryl derivatives **2aX⁻** and are shown in Figure S2 in the Supporting Information. In each case, the anions form hydrogen bonds with three donors: one of the C(α)-H, one *o*-PPh₃ and one *o*-CPh proton. The crystal structures of these salts are worth discussing briefly because of the additional possibility of an interaction of the anion with the second C(α)-H proton of the benzyl group belonging to a second phosphonium ion.

The crystal structure of **1aCl⁻** has been reported previously (Figure 8).^[44] The shortest contact between cation and anion is the interaction of one C(α)-H proton with the chloride anion (H1...Cl distance 2.52 Å and C1-H1...Cl angle 170°), which forms a second hydrogen bond to one of the *o*-PPh₃ protons (H8...Cl distance 2.83 Å and C9-H8...Cl angle 176°) (Table 8). The second C(α)-H proton shows a weaker hydrogen bond to a second chloride anion (H2...Cl distance 2.66 Å, C1-H2...Cl angle 163°), which also has a very short contact to another *o*-PPh₃ proton (H13...Cl distance 2.57 Å, C15-H13...Cl angle 176°). These strong bidirectional interactions result in the formation of one-dimensional chains of alternating cations and anions in the crystal, which interact by weaker contacts between the chloride anions and some of the *p*- and *m*-PPh₃ protons.

The crystal structure of **1aBF₄⁻** with co-crystallized CH₂Cl₂ has previously been reported.^[45] Figure 9 a and b

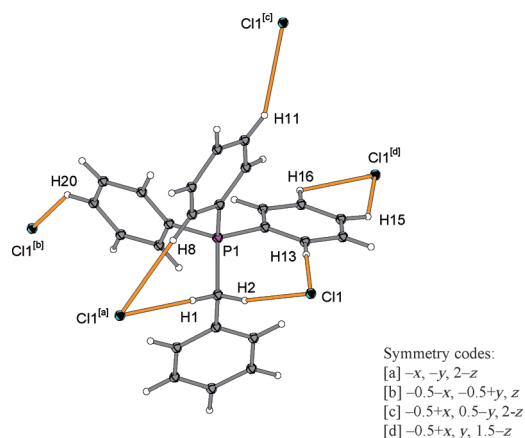


Figure 8. Crystal structure of **1aCl⁻**.^[44] All contacts with $d(\text{H}\cdots\text{X}^-) \leq 2.90$ Å are shown as orange lines. For C-H...X⁻ bond lengths and angles, see Table 8.

compare the structures of **1aBF₄⁻** with co-crystallized CH₂Cl₂^[45] and co-crystallized CHCl₃, respectively. Both structures resemble that of **1aCl⁻** (Figure 8), except that some of the hydrogen bonds are bifurcated towards two of the BF₄⁻ anions' fluorine atoms (Figure 9 and Table 8). On each side of the benzyl moiety, there are strong interactions between the anion and the C(α)-H (H1/H2 in Figure 9 a; H19 A/H19 B in Figure 9 b) and one *p*-PPh₃ proton (H10/H19 in Figure 9 a; H18/H8 in Figure 9 b). The larger size of the BF₄⁻ anion and a slight rotation of the benzyl group's phenyl ring allow for an additional contact between one *o*-CPh proton and one of the BF₄⁻ anions, as shown on the left side in Figure 9 a (H5) and 9 b (H21).

The second BF₄⁻ anion (shown on the right side) cannot undergo such an interaction, because the phenyl ring of the benzyl moiety is already twisted in the wrong direction. Instead, this anion forms strong hydrogen bonds to a solvent molecule. In the case of **1aBF₄⁻·CH₂Cl₂** there is also a contact between an *o*-PPh₃ proton and a chlorine atom of CH₂Cl₂ (Figure 9 a), but this interaction is rather weak (H20...Cl1 distance 2.84 Å, C22-H20...Cl1 angle 135°).

The tetraphenylborate salts: Like **2aBPh₄⁻**, **1aBPh₄⁻** crystallizes as very long fine needles and we could not obtain

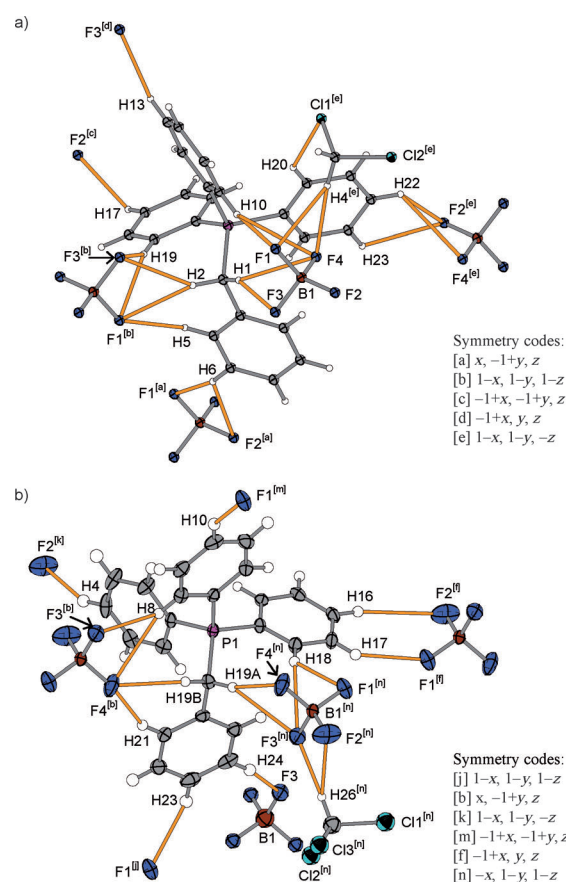


Figure 9. Crystal structures of a) **1aBF₄⁻·CH₂Cl₂** (ref. [45]) and b) **1aBF₄⁻·CHCl₃** (this work). All C-H...X⁻ contacts with $d(\text{H}\cdots\text{X}^-) \leq 2.90$ Å are shown as orange lines. For C-H...X⁻ bond lengths and angles, see Table 8.

Table 8. Distances and angles of C–H...X[−] contacts in crystals of ArCH₂–PPh₃⁺ X[−].

Salt	Donor ^[a]	Acceptor ^[a]	Code ^[a]	<i>d</i> (H...X [−]) [Å]	<i>d</i> (C...X [−]) [Å]	∠(C–H...X [−]) [°]	
1a Cl [−] ^[44b]	H1 (α-H)	Cl1	a	2.52	3.490(6)	170	
	H8	Cl1	a	2.83	3.803(5)	176	
	H2 (α-H)	Cl1	–	2.66	3.602(5)	163	
	H13	Cl1	–	2.57	3.550(6)	176	
	H15	Cl1	d	2.76	3.424(6)	123	
	H16	Cl1	d	2.84	3.472(7)	123	
	H11	Cl1	c	2.87	3.771(7)	153	
	H20	Cl1	b	2.81	3.532(7)	132	
	1a BF ₄ [−] ·CH ₂ Cl ₂ ^[45]	H1 (α-H)	F3	–	2.52	3.437(3)	158
		H1 (α-H)	F4	–	2.81	3.643(3)	145
H10		F1	–	2.49	3.298(2)	146	
H10		F4	–	2.76	3.594(3)	150	
H4 (CH ₂ Cl ₂)		F1	–	2.58	3.367(4)	139	
H4 (CH ₂ Cl ₂)		F4	–	2.52	3.478(5)	169	
H2 (α-H)		F1	b	2.51	3.422(3)	157	
H2 (α-H)		F3	b	2.54	3.403(3)	148	
H19		F1	b	2.57	3.448(2)	157	
H19		F3	b	2.64	3.490(3)	152	
H5		F1	b	2.68	3.391(3)	134	
H6		F1	a	2.56	3.435(3)	158	
H6		F2	a	2.88	3.552(3)	130	
H17		F2	c	2.52	3.283(3)	140	
H13		F3	d	2.65	3.350(3)	133	
H22		F2	e	2.75	3.376(3)	125	
H22		F4	e	2.78	3.398(4)	125	
H23		F2	e	2.80	3.396(3)	123	
H20		Cl1	e	2.84	3.563(3)	135	
1a BF ₄ [−] ·CHCl ₃		H19 A (α-H)	F4	n	2.47	3.390(3)	159
	H19 A (α-H)	F3	n	2.71	3.570(3)	149	
	H18	F3	n	2.82	3.696(3)	154	
	H18	F1	n	2.64	3.412(3)	139	
	H26 (CHCl ₃)	F3	n	2.24(4)	3.192(3)	169(3)	
	H26 (CHCl ₃)	F2	n	2.50(3)	3.250(4)	134(3)	
	H19B (α-H)	F4	b	2.53	3.443(3)	157	
	H8	F4	b	2.83	3.741(4)	162	
	H8	F3	b	2.49	3.253(3)	138	
	H21	F4	b	2.51	3.390(3)	154	
	H24	F3	–	2.60	3.479(4)	153	
	H23	F1	j	2.68	3.226(4)	117	
	H4	F2	k	2.54	3.436(3)	157	
	H10	F1	m	2.87	3.730(4)	151	
	H17	F1	f	2.41	3.209(3)	141	
	H16	F2	f	2.87	3.738(3)	152	
1b BPh ₄ [−]	H1A (α-H)	phenyl ^[b]	–	2.80	3.633(2)	142	
	H1B (α-H)	phenyl ^[c]	d	3.40	4.388(4)	180	

[a] See Figures 8–10 for atom numbering and symmetry codes. [b] Center of six atoms C33, C34, C35, C36, C37, C38. [c] Center of six atoms C27, C28, C29, C30, C31, C32.

suitable material for X-ray structure analyses. We could, however, crystallize (*p*-CF₃-C₆H₄)CH₂–PPh₃⁺BPh₄[−] (**1b**BPh₄[−]) as platelets from CH₂Cl₂/Et₂O. Its crystal structure is shown in Figure 10; the CF₃ group is disordered.

Both C(α)–H bonds (C1–H1A and C1–H1B) point towards phenyl rings of the BPh₄[−] anions. The nature of these C–H...π contacts can be characterized by the distances between the H (or C) atoms and the centers of the phenyl rings, as well as the angles between the C–H bonds and the lines connecting the H atom and the center of the phenyl ring (Table 8). One of the C(α)–H bonds (C1–H1B) points exactly at the center of the phenyl ring of one BPh₄[−] anion (angle: 180°) (Figure 10), but the distance to the center of

the phenyl ring is relatively large (3.40 Å). The second C(α)–H proton (H1A) forms a much closer contact to a phenyl ring of another BPh₄[−] anion (distance: 2.80 Å, sum of C and H van der Waals radii: 2.79 Å^[38]), but in this case the projection of the C(α)–H bond does not point exactly at the phenyl ring (angle 142°).

Comparison of calculated and experimental NMR spectra

We also calculated the ¹H NMR chemical shifts for the ion pairs in CD₂Cl₂ solution with the gauge-independent atomic orbital method (GIAO)^[46] and the functional WP04^[47] (Table 9). This method has been developed especially for the calculation of ¹H NMR data.^[47a] For the calculation of the chemical shifts we additionally used pseudo potentials for all atoms from the third period on.^[43] For a comparison with the experimental data, the δ_H values were averaged for both α-H of the benzyl systems, all *o*-CPh protons, or all six *o*-PPh₃ protons, respectively (Table 9). As the solvent certainly takes part in the hydrogen bond network (compare Figure 9 a), the implicit solvent continuum used for the calculations is a simplification. Further deviations may be caused by the fact that the calculations refer to the most stable conformation, while the experimental data reflect a statistical distribution of different conformations. Still, the experimentally observed trends are fairly well reproduced by the calculated ¹H NMR shifts of the optimized solution structures (Table 9).

Infrared Spectra

Hydrogen bonding is usually associated with red-shifts of the IR stretching frequencies for the involved bonds in the donor group.^[8] Figure 11 shows the C–H stretching regions of the IR spectra of different phosphonium salts in CD₂Cl₂ solution, which were acquired under conditions

where the phosphonium salts are mostly paired (3 × 10^{−2} M solutions).

The red-shifted C(α)–H stretch vibrations ($\bar{\nu} \approx 2831$ and 2791 cm^{−1}) in the benzhydryl triphenylphosphonium halides **2a**Cl[−] and **2a**Br[−] are clearly visible (Figure 11 a). The occurrence of two bands might be explained by couplings with lower-frequency modes, which is a common phenomenon in hydrogen bonding,^[48] or by the existence of two conformations, which are discernible on the IR time scale but not on the NMR time scale. Further investigations are needed to resolve this issue. Unfortunately, direct calculations of the IR bands of ion pairs consisting of such large ions are beyond the scope of this work, since reliable calculations

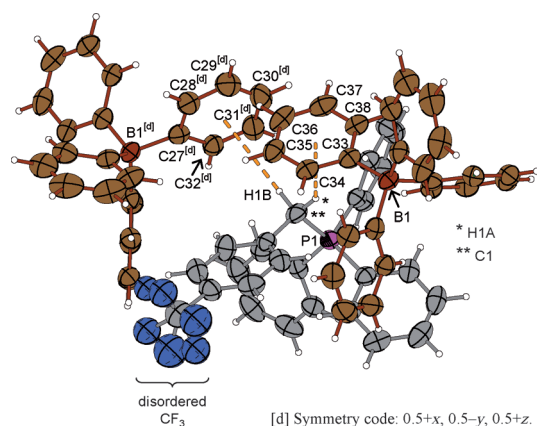


Figure 10. Crystal structure of **1b**BPh₄⁻. For clarity, the carbon atoms of the BPh₄⁻ anions are shown in brown color. The orange dashed lines indicate the distances between the α -protons and the centers of the phenyl groups. For C–H...X⁻ bond lengths and angles, see Table 8.

Table 9. Comparison of calculated and experimental ¹H NMR chemical shifts δ_{H} for **2a**X⁻ and **1a,b**X⁻ in CD₂Cl₂ solution under conditions where the salts exist as ion pairs.

salt	$\delta_{\text{H}}(\text{CHP}^+)^{[a]}$ [ppm]		$\delta_{\text{H}}(o\text{-CPh})^{[a]}$ [ppm]		$\delta_{\text{H}}(o\text{-PPh}_3)^{[a]}$ [ppm]	
	calcd ^[b]	exptl	calcd ^[b]	exptl	calcd ^[b]	exptl
2a Cl ⁻	8.01	8.25	7.43	7.55–7.60	7.54	7.79–7.84
2a Br ⁻	7.71	8.10	7.61	7.53–7.61	7.34	7.74–7.79
2a BF ₄ ⁻	6.57	6.23	7.33	7.19–7.33	6.99	7.43–7.49
2a SbF ₆ ⁻	6.22	5.98	6.98	7.15–7.17	6.95	7.38–7.44
“free” 2a ^[c]	5.84	5.77	6.74	7.09–7.11	6.71	7.33–7.37
1a Cl ⁻	6.33	5.42	7.39	7.07–7.10	7.76	7.70–7.76
1a BF ₄ ⁻	5.04	4.56	6.58	6.91–6.94	7.16	7.48–7.54
“free” 1a ^[c]	4.09	~4.37	6.39	6.87–6.89	6.91	7.43–7.46
1b Br ⁻	5.07	5.78	7.19	7.36	7.33	7.76–7.82
1b BF ₄ ⁻	5.00	4.72	6.78	7.11	7.16	7.54–7.60
“free” 1b ^[c]	4.10	~4.44	6.39	7.04	6.95	7.47–7.51

[a] Averaged δ_{H} of both α protons of the benzyl systems, all six *o*-PPh₃ protons, or all *o*-CPh protons, respectively. [b] From quantum chemical calculations (see text). [c] Experimental values determined from ¹H NMR (600 MHz) spectra of ca. 2×10^{-3} M solutions of the SbF₆⁻, BF₄⁻ and/or BPh₄⁻ salts in CD₂Cl₂. At these concentrations, the phosphonium salts predominantly exist in the form of the free (unpaired) ions.

would require molecular dynamics simulations with the explicit inclusion of at least two solvent shells.

The intensities of the aliphatic C–H stretching bands in the other benzhydryl triphenylphosphonium salts **2a**X⁻ with X⁻ = BF₄⁻, SbF₆⁻, and BPh₄⁻ are very weak (Figure 11 a). These bands can be better discerned in the IR spectra of the benzyl triphenylphosphonium salts **1a**X⁻ (Figure 11 b) and **1b**X⁻ (Figure 11 c). For the halides, we again observe pronounced red-shifts of the C(α)–H stretching bands ($\bar{\nu} \approx 2850$ and 2777 cm^{-1}).

Interestingly, the C(α)–H bands of the tetrafluoroborates **1a,b**BF₄⁻ ($\bar{\nu} \approx 2962$ and 2919 cm^{-1}) in Figure 11 b and 11 c are located at higher wave numbers (i.e., blue-shifted) and have lower intensities than those of the corresponding tetraphenylborates **1a,b**BPh₄⁻ ($\bar{\nu} \approx 2935$ and 2899 cm^{-1}), although the dissociation constants K_{D} indicate stronger interactions of the phosphonium ions with the BF₄⁻ anions than

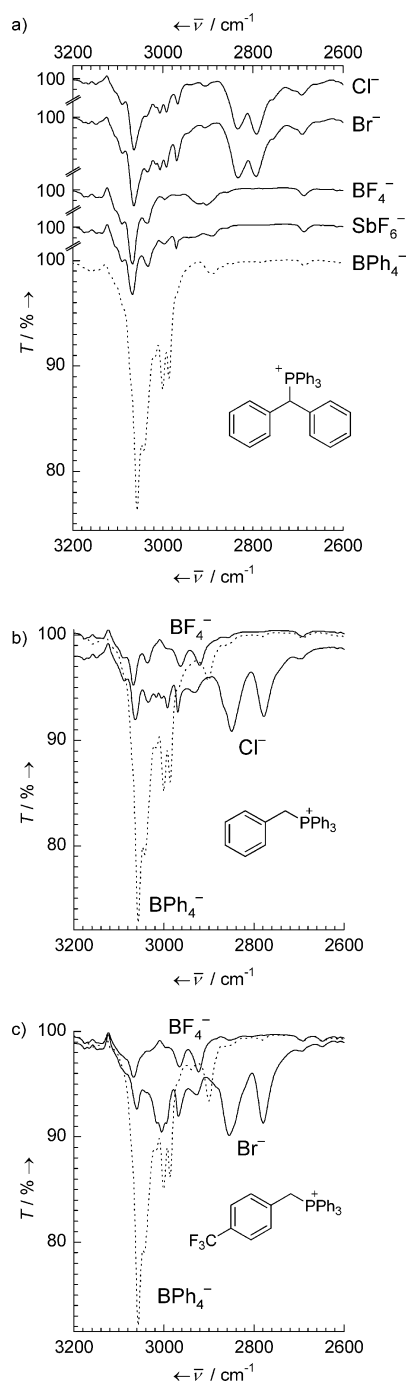


Figure 11. IR spectra of 3×10^{-2} M solutions of a) **2a**X⁻ (vertical offset for visibility), b) **1a**X⁻, or c) **1b**X⁻ with X⁻ = Cl⁻, Br⁻, BF₄⁻, SbF₆⁻, or BPh₄⁻ in CD₂Cl₂.

with the BPh₄⁻ anions (Table 4). This may indicate the existence of so-called blue-shifting hydrogen bonds between the phosphonium ions and the BF₄⁻ anions (see below).

As both the NMR and X-ray data indicated hydrogen bonding between the counter-anions and aryl protons (see above), it is also interesting to compare the aromatic C–H stretching vibrations. Indeed, the C(aryl)–H stretching bands of the BF₄⁻ salts are found above 3000 cm^{-1} , while those of the halides extend further into the red to well

below 3000 cm⁻¹ (Figure 11 a–c). The IR spectra thus provide further evidence for C(aryl)–H...X⁻ hydrogen bonds in CD₂Cl₂ solutions of the phosphonium halides.

C–H...X⁻ Hydrogen Bonds: What Is Typical?

Bird's eye view of the whole data set

The NMR data of the phosphonium salts in CD₂Cl₂ solution show that ion pairing with the counteranion X⁻ mainly affects the proton resonances of the C(α)–H, *o*-PPh₃, and *o*-CPh protons of **2a** (Table 1) or **1a** (Table 3), respectively. A comparison with the crystal structures of these salts reveals that these protons are also involved in the shortest and least bent C–H...X⁻ contacts in the crystals (Figure 7–9; Tables 7 and 8). The presence of C–H...X⁻ hydrogen bonds in solutions of **2X⁻** and **1X⁻** is consistent with the strong deshielding of the respective protons, as well as with the fact that the deshielding increases with increasing C–H acidity and with increasing basicity of the anions X⁻ (SbF₆⁻ < BF₄⁻ < Br⁻ < Cl⁻).^[34] Moreover, the IR spectra clearly show that the C–H stretch frequencies of the phosphonium salts in CD₂Cl₂ solution depend on the counter-anion (Figure 11). The results of our quantum chemical calculations also confirm C–H...X⁻ hydrogen bonds for the C(α)–H, *o*-PPh₃, and *o*-CPh protons of **2aX⁻** and **1a,bX⁻** ion pairs in CH₂Cl₂ solution (Figure 7 a–d; Tables 6 and 9). The relevant data for the C(α)–H...X⁻ hydrogen bonds in dichloromethane solution are summarized again in Tables 10 and 11.

The data presented in the three previous Sections as a whole thus clearly support the existence of C–H...X⁻ hydrogen bonds between the phosphonium ions and the anions (Tables 10 and 11). Some of these C–H...X⁻ interactions, however, show spectroscopic characteristics which are worth discussing in greater detail in the following. Looking at

these pieces of evidence individually, one might not have recognized the hydrogen bonds clearly in some cases.

The nature of the “BPh₄⁻ Effect” in benzyl triphenylphosphonium salts

While we did not find such interactions in **2a**BPh₄⁻, the crystallographic data in Figure 10 reveal C–H...π interactions between **1b** and BPh₄⁻, where the protons reside above the centers of the phenyl rings. Unlike the typical CH–π interaction, which is mainly based on dispersion interactions,^[49] the interaction between **1b** and BPh₄⁻ can be expected to have a strong electrostatic component due to the high acidity of the C–H bond and the negative charge on the phenyl rings of the BPh₄⁻ anion. This notion is supported by the strong directionality of the C1–H1B...Ph interaction, since the electrostatic interaction is the main source of directionality in CH–π interactions.^[49] Hence, the C(α)–H...Ph interactions in **1b** BPh₄⁻ can be viewed as hydrogen bonds in which a phenyl ring of the tetraphenylborate anion acts as the hydrogen bond acceptor.^[2,50] Similar C(α)–H...Ph hydrogen bonds have also been reported in the crystal structure of choline tetraphenylborate, Me₃N⁺–C(α)H₂–CH₂OH BPh₄⁻ (H...Ph distances 2.42 Å and 2.38 Å, C–H...Ph angles 168 and 159°).^[50b]

A similar interaction between cation and anion in CD₂Cl₂ solution can explain the upfield shift of the C(α)–H resonances of **1a,b**BPh₄⁻ in the ¹H NMR spectra (Figure 2): The resulting ring current effect^[51] over-compensates any small downfield shift in the ¹H NMR spectrum that may be expected due to the formation of a weak hydrogen bond.

Blue-shifting hydrogen bonds with weak hydrogen bond acceptors

Blue-shifting hydrogen bonds show stretching vibrations at higher wave numbers, often accompanied by reduced inten-

Table 10. Summary of experimental and calculated data for the C(α)–H...X⁻ hydrogen bonds of the benzhydryl triphenylphosphonium ion pairs **2aX⁻** in dichloromethane solution.

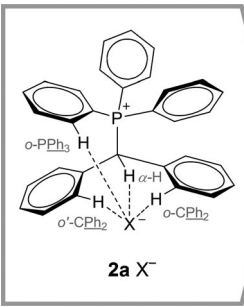
	X ⁻	Cl ⁻	Br ⁻	BF ₄ ⁻	SbF ₆ ⁻	BPh ₄ ⁻ (≈ free ion)	free ion	
 <p>2aX⁻</p>	δ _H for C(α)–H [ppm]	8.25	8.10	6.23	5.98	5.72	5.77	
	¹ J _{C,H} for C(α)–H [Hz]	131.3	131.1	130.2	129.3	128.7	n/a	
	$\tilde{\nu}_{\text{CH}}$ [cm ⁻¹]	2832 (s) 2791 (s)	2829 (s) 2791 (s)	2903 (w) 2918 (w)	2889 (w)	2888 (w)	n/a	
	calcd <i>d</i> (C–H) [Å]	1.1022	1.1021	1.0968	1.0977	n/a	1.0977	
	calcd <i>d</i> (H...X ⁻) [Å]	2.44	2.64	2.30/2.20	2.28/2.44	n/a	–	
	calcd <i>d</i> (C...X ⁻) [Å]	3.54	3.74	3.24/3.23	3.28/3.37	n/a	–	
	calcd ∠(C–H...X ⁻) [°]	176	177	142/156	151/141	n/a	–	
	further H-bonds to... (also see Figure 7 a–d)		H2 (<i>o</i> -PPh ₃) H31 (<i>o</i> -CPh) H21 (<i>o'</i> -CPh ₂)	H6 (<i>o</i> -PPh ₃) H25 (<i>o</i> -CPh ₂) H13 (<i>o'</i> -CPh ₂)	H12 (<i>o</i> -PPh ₃) H31 (<i>o</i> -CPh ₂) H25 (<i>o'</i> -CPh ₂)	H2 (<i>o</i> -PPh ₃) H21 (<i>o</i> -CPh ₂) H15 (<i>o'</i> -CPh ₂) H3 (<i>m</i> -PPh ₃)	n/a	–

Table 11. Summary of experimental and calculated data for the C(α)–H \cdots X $^-$ hydrogen bonds of the benzyl triphenylphosphonium ion pairs **1a**X $^-$ in dichloromethane solution.

	X $^-$		Br $^-$		BF $_4^-$		BPh $_4^-$		free ions	
	1a	1b	1a	1a	1b	1a	1b	1a	1b	
δ_{H} for C(α)–H [ppm]	5.42	5.78	4.56	4.72	3.94	3.66	–4.37	–4.44		
$^1J_{\text{C,H}}$ for C(α)–H [Hz]	134.6	134.6	134.2	134.9	133.9	134.6	n/a	n/a		
$\bar{\nu}_{\text{CH}}$ [cm $^{-1}$]		2852 (s) 2776 (s)	2848 (s) 2778 (s)	2960 (m) 2916 (m)	2963 (m) 2921 (m)	2899 (m)	2935 (w) 2899 (m)	n/a	n/a	
calcd $d(\text{C–H})^{[a]}$ [Å]		1.0983	1.0980	1.0929	1.0931	n/a	n/a	1.0941 ^[b]	1.0940 ^[b]	
calcd $d(\text{H}\cdots\text{X}^-)$ [Å]		2.52	2.72	2.18/2.34	2.15/2.34	n/a	n/a	–	–	
calcd $d(\text{C}\cdots\text{X}^-)$ [Å]		3.57	3.74	3.26/3.12	3.22/3.14	n/a	n/a	–	–	
calcd $\angle(\text{C–H}\cdots\text{X}^-)$ [°]		159	154	172/126	168/128	n/a	n/a	–	–	
further H-bonds to...		<i>o</i> -PPh $_3$ <i>o</i> -CPh	n/a	n/a	–	–				

[a] Length of C(α)–H bond acting as hydrogen bond donor. [b] Average of two C(α)–H bonds of the free phosphonium ions **1a** (± 0.0007 Å) or **1b** (± 0.0008 Å), respectively.

sities of the IR bands,^[52,53] which is the opposite behavior of normal hydrogen bonds.^[8] The nature of blue-shifting hydrogen bonds has been discussed controversially,^[52,53] but now there seems to be a general agreement that there is no fundamental difference between blue-shifting and normal red-shifting hydrogen bonds.^[54]

According to Joseph and Jemmis,^[53] there are two opposing effects, when the hydrogen bond acceptor X $^-$ approaches the C–H proton. On the one hand, there is an attractive interaction between the positive H and the negative X $^-$, which lengthens the C–H bond and reduces the force constant. On the other hand, the presence of X $^-$ induces a greater polarization of the C–H bond, because it compensates the resulting positive charge at H. As a result, the C–H bond is contracted and the force constant increases. If the former effect dominates, a classical red-shifting hydrogen bond is the result. If the latter dominates, a blue-shift of the frequency of the C–H stretch mode is observed.^[53]

Compared to classical hydrogen bond donors such as O–H or N–H, the C–H bond is longer and less polar. An approach of the hydrogen bond acceptor X $^-$ will thus lead to a considerable polarization of the C–H bond. Whether the increased polarization causes a contraction of the C–H bond and a blue shift of its IR stretching band depends on the relative importance of the compensating attractive interaction between H and X $^-$. Increasing interaction energy between the hydrogen bond donor and acceptor causes a blue shift at relatively long equilibrium distances between H and X $^-$, which then decreases again and changes into a red shift as the equilibrium distance between H and X $^-$ becomes shorter.^[53] For strong acceptors such as Cl $^-$ or Br $^-$, the attraction between H and X $^-$ clearly dominates and we observe the classical red-shifting hydrogen bonds (Figure 11, Tables 10 and 11). The hydrogen bond acceptor BF $_4^-$ seems to be of an intermediate strength, where we observe a blue shift with the C–H hydrogen bond donors **1a** and **1b** in CD $_2$ Cl $_2$ solution (Figure 11 b and c, Table 11).

This interpretation of the IR spectra is supported by the quantum chemical calculations, which also show C(α)–H bond contractions (ca. -1 mÅ) relative to the unpaired phosphonium ions for the tetrafluoroborate salts and bond elongations (ca. $+4$ mÅ) for the halide salts (Tables 10 and 11). An experimental confirmation of the polarization of the C(α)–H bond, which is expected for both red- and blue-shifting hydrogen bonds (see above), is provided by the NMR data of **2a** X $^-$ (Table 1) and **1a** X $^-$ (Table 3): Compared to the free ions, the H atoms are deshielded (i.e., lower electron density around H) and the C atoms are shielded (i. e., higher electron density around C) in the hydrogen-bonded systems. While δ_{H} may reflect changes in the electron density caused by polarization of the C–H bond as well as by interaction with the acceptor X $^-$, changes in δ_{C} primarily reflect polarization effects. This polarization is observed in all studied systems and becomes more pronounced with increasing interaction between cation and anion (Tables 1 and 3).

Cooperativity or anti-cooperativity phenomena between the different types of hydrogen bonds may also play a role in controlling the strengths of the C–H \cdots X $^-$ hydrogen bonds.^[55] A point which may be relevant here is the fact that the hydrogen bonds involving the BF $_4^-$ and SbF $_6^-$ acceptors, which are characterized as blue-shifting in this work, are bifurcated hydrogen bonds (Figures 7 and 9). A theoretical study of linear and bifurcated hydrogen bonds between the proton donors H $_2$ CZ (Z=O, S, Se) or H $_2$ CZ $_2$ (Z=F, Cl, Br) and the halide ions Cl $^-$ and Br $^-$ found that all linear hydrogen bonds in the investigated systems were red-shifting, while all bifurcated hydrogen bonds were blue-shifting.^[56]

The NMR data for the phosphonium ion pairs **2a**X $^-$ (Table 1) or **1a**X $^-$ (Table 3) do not show any qualitative differences between the blue-shifting and red-shifting hydrogen bonds. We note that in both the blue-shifting (**2a**BPh $_4^- \approx$ “free” **2a** \rightarrow **2a**BF $_4^-$) as well as the red-shifting series (**2a**Br $^- \rightarrow$ **2a**Cl $^-$) of the benzhydryl triphenylphosphonium salts, the chemical shifts δ_{C} for the α -carbon atom of **2a** de-

crease (Table 1) and the coupling constants $^1J_{\text{HC}}$ for the C(α)-H bond increase (Table 10) with increasing interaction energy. These parameters had previously been suggested as indicators for the transition between blue- and red-shifting hydrogen bonds, based on data for a series of single hydrogen bonds between fluoroform and various hydrogen bond acceptors.^[57]

Implications for the identification of C-H...X⁻ hydrogen bonds

In the course of this work, we have encountered many of the concepts that have been debated controversially in the field of hydrogen bonding during the last decades: hydrogen bonds involving C-H donors, bi- and multi-furcated hydrogen bonds, "aromatic" hydrogen bonds with phenyl groups as acceptors, and "improper" blue-shifting hydrogen bonds. It seems that these are widespread phenomena which should be considered when dealing with solutions of onium salts. As hydrogen bonding can lead to both downfield or upfield shifts in the ^1H NMR spectra, and both red- or blue-shifts in the IR stretching bands, none of these techniques alone is sufficient to unambiguously detect weak C-H...X⁻ interactions in solution. The combination of these methods with variations of concentrations, C-H acidities, or X⁻ basicities provides more detailed insights.

Conclusion

The remarkably large counterion-induced shifts in the ^1H NMR spectra of the phosphonium ion Ph₂CH-PPh₃⁺ (**2a**) (e.g., C(α)-H signals of **2a**Cl⁻: 8.25 ppm; **2a**BPh₄⁻: 5.72 ppm in CD₂Cl₂) have previously been attributed mainly to the shielding by the ring current effect of the BPh₄⁻ anions.^[9] In contrast, we have now demonstrated that the ^1H NMR spectrum of the phosphonium ion **2a** is not affected by BPh₄⁻ anions at all, and that the formation of ion pairs of **2a** with Cl⁻ anions or other hydrogen bond acceptors is responsible for the large downfield shifts of the C(α)-H signals of **2a** in CD₂Cl₂ relative to that of the unpaired cation (Figure 1, Table 10). Even weakly coordinating anions such as SbF₆⁻ or BF₄⁻ induce a noticeable downfield shift of +0.2 to +0.4 ppm. In sterically less congested systems such as PhCH₂-PPh₃⁺ (**1a**), the BPh₄⁻ anion does induce a noticeable upfield shift, but its magnitude remains second to the deshielding effect of Cl⁻ or Br⁻ anions (Figure 2, Table 11).

The counterion-induced NMR shifts in quaternary phosphonium salts are caused by the formation of charge-assisted C-H...X⁻ hydrogen bonds between the anion and the C(α)-H protons of the cation. The *o*-PPh₃ and *o*-CPh protons are likewise involved in such C-H...X⁻ hydrogen bonds. The strengths of the hydrogen bonds increase in the order BPh₄⁻ < SbF₆⁻ < BF₄⁻ < Br⁻ < Cl⁻ and also increase with increasing C-H-acidities of the phosphonium ions. A C-H... π hydrogen bond between C(α)-H and the BPh₄⁻

anion has also been observed in the crystal structure of **1b**BPh₄⁻, and the NMR spectra indicate that a similar interaction is also relevant in dichloromethane solution. Ion pairing thus plays an important role in solutions of phosphonium salts even when weakly coordinating anions such as BF₄⁻, SbF₆⁻, or BPh₄⁻ are employed in solvents such as CH₂Cl₂ or CHCl₃. In more polar solvents such as CH₃CN, only stronger hydrogen-bond acceptors such as Cl⁻ or Br⁻ form ion pairs with the phosphonium ions.

Similar C-H...X⁻ hydrogen bonds probably also play a major role in solutions of other onium salts, as demonstrated by the large number of examples for the "BPh₄⁻ effect" in phosphonium,^[9,10] ammonium,^[14] anilinium,^[11] pyridinium,^[13] sulfonium,^[15] arsonium,^[12] and stibonium^[12] salts, which were collected by Schiemenz and co-workers. Indeed, the crystal structures reported for tetraarylborate salts of other onium ions^[50b,c] show similar cation-anion interactions as described for **1b**BPh₄⁻ in this work (Figure 10). However, if the conclusions drawn for the benzyl triphenylphosphonium salts **1a,b**X⁻ in this work are also applicable to these other onium salts, the strongest anion effect has to be expected for the "ordinary" halide salts and not the BPh₄⁻ salts. The fact that red-shifts of the C(α)-H IR stretching bands in CHCl₃ solution were reported even for *alkyl* triphenylphosphonium halides^[7] illustrates that hydrogen bonding also plays a role for substrates of lower C-H acidity.

This work once again demonstrates that the formation of weak hydrogen bonds does not always induce red-shifts of the C-H stretch vibrations. This may be a reason why the decisive role of hydrogen bonding for the structure of onium ion pairs has often been underappreciated in the past, although the structural features of the ion pairs control the spectroscopic characteristics and reactivities of the onium salts in solution.^[59]

Experimental Section

Syntheses of the phosphonium salts ArCH₂-PPh₃⁺X⁻ (1X⁻), Ar₂CH-PPh₃⁺X⁻ (2X⁻), and Ar₂CH-P(*p*-Cl-C₆H₄)₃⁺X⁻ (3X⁻): The benzyl triphenylphosphonium salts **1a**Cl⁻ and **1a**BF₄⁻ are commercially available; **1b**Br⁻ was prepared by a literature method;^[58] **1b**BF₄⁻ and **1a,b**BPh₄⁻ were prepared by anion exchange from **1a**Cl⁻ or **1b**Br⁻. The benzhydryl triphenylphosphonium tetrafluoroborates Ar₂CH-PPh₃⁺BF₄⁻ (**2**BF₄⁻) and **2a**Cl⁻ were synthesized by heating the benzhydrols Ar₂CH-OH (**4**) with Ph₃PH⁺X⁻ (X⁻=BF₄⁻ or Cl⁻). The phosphonium bromides Ar₂CH-PAr₃⁺Br⁻ (**2**Br⁻ and **3**Br⁻) were obtained by reaction of the benzhydryl bromides Ar₂CH-Br (**5**) with PAr₃. Subsequent anion metathesis provided the phosphonium salts **2**SbF₆⁻, **2**BPh₄⁻, **3**BF₄⁻, and **3**SbF₆⁻. Details of the synthetic procedures are described in the Supporting Information.

Calculated structures of phosphonium salts in solution: The solution structures of the salts **1a,b**X⁻ and **2a**X⁻ were obtained by DFT calculations using the program package Gaussian09.^[39] The solution structures of the BPh₄⁻ salts were not calculated due to the large size of the ions. The geometries of the different ion pairs **1a,b**X⁻ and **2a**X⁻ were optimized and confirmed by frequency analysis showing no imaginary frequency. We used the recently developed hybrid meta-GGA functional M06-2X for all geometry optimizations,^[40] which has been shown to describe intermolecular interactions adequately.^[40] We included implicit sol-

vent effects of dichloromethane using the integral equation formalism variant of the polarizable continuum model (IEFPCM).^[41] The optimizations were calculated with the double ζ basis 6-31+G(d,p).^[42] For all atoms in the fourth period and higher we used effective core potentials.^[43] Details of the calculations and the calculated structures are given in Section S4 of the Supporting Information.

Crystal structure determinations: CCDC-916846 (**1a**BF₄⁻·CHCl₃), -916530 (**1b**BPh₄⁻), -916849 (**2a**Cl⁻), -916848 (**2a**Br⁻), -916847 (**2a**BF₄⁻) and -916850 (**2a**SbF₆⁻) contain the supplementary crystallographic data for this paper. These data can be obtained free of charge from The Cambridge Crystallographic Data Centre via www.ccdc.cam.ac.uk/data_request/cif.

Acknowledgements

We thank Claudia Dubler and Dr. David Stephenson for assistance with the NMR experiments, one anonymous reviewer for the thorough discussion and many helpful suggestions, and the Deutsche Forschungsgemeinschaft (SFB 749, Teilprojekt B1) for financial support.

- [1] a) G. R. Desiraju, *Acc. Chem. Res.* **1991**, *24*, 290–296; b) G. R. Desiraju, *Acc. Chem. Res.* **1996**, *29*, 441–449; c) M. C. Wahl, M. Sundaralingam, *Trends Biochem. Sci.* **1997**, *22*, 97–102; d) R. K. Castellano, *Curr. Org. Chem.* **2004**, *8*, 845–865; e) H.-J. Schneider, *Angew. Chem.* **2009**, *121*, 3982–4036; *Angew. Chem. Int. Ed.* **2009**, *48*, 3924–3977; f) Y. Hua, A. H. Flood, *Chem. Soc. Rev.* **2010**, *39*, 1262–1271; g) J. J. Novoa, F. Mota, E. D’Oria, in *Hydrogen Bonding—New Insights* (Ed.: S. J. Grabowski), Springer, Dordrecht, **2006**, pp. 193–244; h) S. Scheiner, in *Hydrogen Bonding—New Insights* (Ed.: S. J. Grabowski), Springer, Dordrecht, **2006**, pp. 263–292; i) W. A. Herrebout, M. A. Suhm, *Phys. Chem. Chem. Phys.* **2011**, *13*, 13858–13859; j) S. Scheiner, *Phys. Chem. Chem. Phys.* **2011**, *13*, 13860–13872.
- [2] a) M. Nishio, *CrystEngComm* **2004**, *6*, 130–158; b) M. Nishio, *Phys. Chem. Chem. Phys.* **2011**, *13*, 13873–13900.
- [3] T. Steiner, *Angew. Chem.* **2002**, *114*, 50–80; *Angew. Chem. Int. Ed.* **2002**, *41*, 48–76.
- [4] a) B. P. Hay, V. S. Bryantsev, *Chem. Commun.* **2008**, 2417–2428; b) L. Pedzisa, B. P. Hay, *J. Org. Chem.* **2009**, *74*, 2554–2560.
- [5] Y. Fu, H.-J. Wang, S.-S. Chong, Q.-X. Guo, L. Liu, *J. Org. Chem.* **2009**, *74*, 810–819.
- [6] J.-P. Cheng, B. Liu, Y. Zhao, Y. Sun, X.-M. Zhang, Y. Lu, *J. Org. Chem.* **1999**, *64*, 604–610.
- [7] L. B. Senyavina, V. I. Sheichenko, Y. N. Sheinker, A. V. Dombrovskii, M. I. Shevchuk, L. I. Barsukov, L. D. Bergel’son, *Zh. Obshch. Khim.* **1967**, *37*, 499–506; *J. Gen. Chem. USSR* **1967**, *37*, 469–474.
- [8] E. Arunan, G. R. Desiraju, R. A. Klein, J. Sadlej, S. Scheiner, I. Alkorta, D. C. Clary, R. H. Crabtree, J. J. Dannenberg, P. Hobza, H. G. Kjaergaard, A. C. Legon, B. Mennucci, D. J. Nesbitt, *Pure Appl. Chem.* **2011**, *83*, 1637–1641.
- [9] G. P. Schiemenz, *J. Magn. Reson.* **1972**, *6*, 291–297.
- [10] G. P. Schiemenz, E. Papageorgiou, *Phosphorus Sulfur* **1982**, *13*, 41–58.
- [11] G. P. Schiemenz, *Org. Magn. Reson.* **1973**, *5*, 257–261.
- [12] G. P. Schiemenz, *J. Organomet. Chem.* **1973**, *52*, 349–354.
- [13] G. P. Schiemenz, *J. Mol. Struct.* **1973**, *16*, 99–102.
- [14] G. P. Schiemenz, *Tetrahedron* **1973**, *29*, 741–745.
- [15] G. P. Schiemenz, H. P. Hansen, *Angew. Chem.* **1973**, *85*, 404; *Angew. Chem. Int. Ed. Engl.* **1973**, *12*, 400.
- [16] Recent examples where this view was expressed: a) G. P. Schiemenz, C. Näther, S. Pörksen, *Z. Naturforsch. B: Chem. Sci.* **2003**, *58*, 59–73; b) G. P. Schiemenz, *Magn. Reson. Chem.* **2010**, *48*, 261–269.
- [17] Also see: R. P. Taylor, I. D. Kuntz, Jr., *J. Am. Chem. Soc.* **1970**, *92*, 4813–4823. In this study, an upfield shift of $\Delta\delta_{\text{H}} \approx -0.4$ ppm was observed for the methyl protons of CH₃PPh₃⁺X⁻ in CDCl₃ solution, when the anion X⁻ was varied from chloride to picrate. The fact that the same anion variation caused much larger upfield shifts in aromatic solvents (e.g., $\Delta\delta_{\text{H}} \approx -1.6$ ppm in 1-bromonaphthalene) was explained by the ability of the smaller anions to form contact pairs with the onium ions, thus preventing the interaction of the aromatic solvent with the α protons of the cation.
- [18] a) G. P. Schiemenz, *Angew. Chem.* **1971**, *83*, 929–930; *Angew. Chem. Int. Ed. Engl.* **1971**, *10*, 855; b) G. P. Schiemenz, H. Rast, *Tetrahedron Lett.* **1972**, *13*, 1697–1700; c) G. P. Schiemenz, P. Klemm, *Org. Magn. Reson.* **1974**, *6*, 276–278.
- [19] J. Ammer, C. F. Sailer, E. Riedle, H. Mayr, *J. Am. Chem. Soc.* **2012**, *134*, 11481–11494.
- [20] J. Ammer, C. Nolte, H. Mayr, *J. Am. Chem. Soc.* **2012**, *134*, 13902–13911.
- [21] a) C. K. Broder, M. G. Davidson, V. T. Forsyth, J. A. K. Howard, S. Lamb, S. A. Mason, *Cryst. Growth Des.* **2002**, *2*, 163–169; b) I. Ling, Y. Alias, A. N. Sobolev, C. L. Raston, *CrystEngComm* **2010**, *12*, 4321–4327.
- [22] a) A. Hamdi, K. C. Nam, B. J. Ryu, J. S. Kim, J. Vicens, *Tetrahedron Lett.* **2004**, *45*, 4689–4692; b) H. M. Yeo, B. J. Ryu, K. C. Nam, *Org. Lett.* **2008**, *10*, 2931–2934; c) H. M. Yeo, N. J. Jeon, K. C. Nam, *Bull. Korean Chem. Soc.* **2011**, *32*, 3171–3174; d) W. Huang, H. Lin, H. Lin, *Sens. Actuators B* **2011**, *153*, 404–408.
- [23] Ionic liquids: D. R. MacFarlane, M. Forsyth, E. I. Izgorodina, A. P. Abbott, G. Annat, K. Fraser, *Phys. Chem. Chem. Phys.* **2009**, *11*, 4962–4967.
- [24] Deep eutectic solvents: a) M. A. Kareem, F. S. Mjalli, M. A. Hashim, I. M. AlNashef, *J. Chem. Eng. Data* **2010**, *55*, 4632–4637; b) K. Shahbaz, F. S. Mjalli, M. A. Hashim, I. M. AlNashef, *Energy Fuels* **2011**, *25*, 2671–2678.
- [25] a) E. O. Alonso, L. J. Johnston, J. C. Scaiano, V. G. Toscano, *Can. J. Chem.* **1992**, *70*, 1784–1794; b) C. Imrie, T. A. Modro, E. R. Rohwer, C. C. P. Wagener, *J. Org. Chem.* **1993**, *58*, 5643–5649.
- [26] a) G. P. Schiemenz, M. Sommerfeld, *Phosphorus Sulfur* **1979**, *6*, 273–274; b) G. P. Schiemenz, R. Hinz, *Phosphorus Sulfur* **1983**, 237–240; c) G. P. Schiemenz, R. Bukowski, L. Eckholtz, B. Varnskühler, *Z. Naturforsch. B Chem. Sci.* **2000**, *55*, 12–20; d) G. P. Schiemenz, C. Näther, S. Pörksen, *Z. Naturforsch. B Chem. Sci.* **2003**, *58*, 663–671.
- [27] Counteranion effects in the Wittig reaction: a) H. Bandmann, T. Bartik, S. Bauckloh, A. Behler, F. Brille, P. Heimbach, J.-W. Louven, P. Ndalut, H.-G. Preis, E. Zeppenfeld, *Z. Chem.* **1990**, *30*, 193–204; b) H. Yung-Son, C.-F. Lee, *Tetrahedron* **2000**, *56*, 7893–7902.
- [28] Reviews about phosphonium salts as organocatalysts: a) T. Werner, *Adv. Synth. Catal.* **2009**, *351*, 1469–1481; b) D. Enders, T. V. Nguyen, *Org. Biomol. Chem.* **2012**, *10*, 5327–5331; c) D. Uraguchi, T. Ooi, *Yuki Gosei Kagaku Kyokaiishi* **2010**, *68*, 1185–1194.
- [29] F. G. Bordwell, *Acc. Chem. Res.* **1988**, *21*, 456–463.
- [30] Y. Marcus, *Pure Appl. Chem.* **1983**, *55*, 977–1021.
- [31] H. Friebolin, *Basic One- and Two-Dimensional NMR Spectroscopy*, 5th ed., Wiley-VCH, Weinheim, **2011**, p. 97.
- [32] R. H. Contreras, J. E. Peralta, *Prog. Nucl. Magn. Reson. Spectrosc.* **2000**, *37*, 321–425.
- [33] R. K. Harris, in *Encyclopedia of Nuclear Magnetic Resonance*, Vol. 5 (Eds.: D. M. Grant, R. K. Harris), Wiley, Chichester, **1996**, pp. 3301–3314.
- [34] I. A. Koppel, P. Burk, I. Koppel, I. Leito, T. Sonoda, M. Mishima, *J. Am. Chem. Soc.* **2000**, *122*, 5114–5124.
- [35] H. Mayr, A. R. Ofial, E.-U. Würthwein, N. C. Aust, *J. Am. Chem. Soc.* **1997**, *119*, 12727–12733.
- [36] R. Schneider, H. Mayr, P. H. Plesch, *Ber. Bunsen-Ges.* **1987**, *91*, 1369–1374.
- [37] C. Hansch, A. Leo, R. W. Taft, *Chem. Rev.* **1991**, *91*, 165–195.
- [38] a) van der Waals radii of C (1.70 Å), F (1.47 Å), Cl (1.75 Å), Br (1.85 Å) taken from: A. Bondi, *J. Phys. Chem.* **1964**, *68*, 441–451; b) radius of hydrogen (1.09 Å) taken from: R. S. Rowland, R. Taylor, *J. Phys. Chem.* **1996**, *100*, 7384–7391.
- [39] Gaussian 09, Revision A.02, M. J. Frisch, G. W. Trucks, H. B. Schlegel, G. E. Scuseria, M. A. Robb, J. R. Cheeseman, G. Scalmani, V.

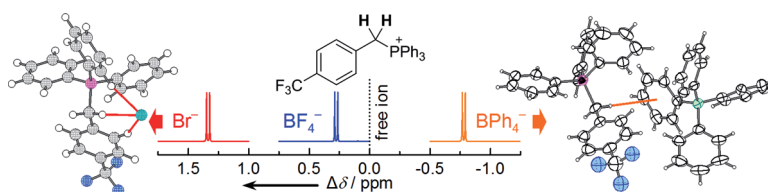
- Barone, B. Mennucci, G. A. Petersson, H. Nakatsuji, M. Caricato, X. Li, H. P. Hratchian, A. F. Izmaylov, J. Bloino, G. Zheng, J. L. Sonnenberg, M. Hada, M. Ehara, K. Toyota, R. Fukuda, J. Hasegawa, M. Ishida, T. Nakajima, Y. Honda, O. Kitao, H. Nakai, T. Vreven, J. A. Montgomery Jr., J. E. Peralta, F. Ogliaro, M. Bearpark, J. J. Heyd, E. Brothers, K. N. Kudin, V. N. Staroverov, R. Kobayashi, J. Normand, K. Raghavachari, A. Rendell, J. C. Burant, S. S. Iyengar, J. Tomasi, M. Cossi, N. Rega, J. M. Millam, M. Klene, J. E. Knox, J. B. Cross, V. Bakken, C. Adamo, J. Jaramillo, R. Gomperts, R. E. Stratmann, O. Yazyev, J. Austin, R. Cammi, C. Pomelli, J. W. Ochterski, R. L. Martin, K. Morokuma, V. G. Zakrzewski, G. A. Voth, P. Salvador, J. J. Dannenberg, S. Dapprich, D. A. Daniels, O. Farkas, J. B. Foresman, J. V. Ortiz, J. Cioslowski, D. J. Fox, Gaussian, Inc., Wallingford CT, **2009**.
- [40] Y. Zhao, D. G. Truhlar, *Theor. Chem. Acc.* **2008**, *120*, 215–241.
- [41] a) M. Caricato, B. Mennucci, J. Tomasi, F. Ingrosso, R. Cammi, S. Corni, G. Scalmani, *J. Chem. Phys.* **2006**, *124*, 124520; b) R. Impropa, V. Barone, G. Scalmani, M. J. Frisch, *J. Chem. Phys.* **2006**, *125*, 054103; c) G. Scalmani, M. J. Frisch, *J. Chem. Phys.* **2010**, *132*, 114110.
- [42] a) R. Ditchfield, *J. Chem. Phys.* **1971**, *54*, 724–728; b) P. C. Hariharan, J. A. Pople, *Theor. Chim. Acta* **1973**, *28*, 213–222; c) V. A. Ras-solov, M. A. Ratner, J. A. Pople, P. C. Redfern, L. A. Curtiss, *J. Comput. Chem.* **2001**, *22*, 976–984.
- [43] a) A. Bergner, M. Dolg, W. Küchle, H. Stoll, H. Preuß, *Mol. Phys.* **1993**, *80*, 1431–1441; b) B. Metz, H. Stoll, M. Dolg, *J. Chem. Phys.* **2000**, *113*, 2563–2569.
- [44] a) A. C. Skapski, F. A. Stephens, *J. Cryst. Mol. Struct.* **1974**, *4*, 77–85; b) A. Fischer, D. Wiebelhaus, *Z. Kristallogr. New Cryst. Struct.* **1997**, *212*, 335–336.
- [45] M. C. Ramirez de Arellano, private communication, **1997**, CCDC-100328.
- [46] a) R. Ditchfield, *Mol. Phys.* **1974**, *27*, 789–807; b) F. London, *J. Phys. Radium* **1937**, *8*, 397–409; c) K. Wolinski, J. F. Hinton, P. Pulay, *J. Am. Chem. Soc.* **1990**, *112*, 8251–8260.
- [47] a) K. W. Wüthala, T. R. Hoye, C. J. Cramer, *J. Chem. Theory Comput.* **2006**, *2*, 1085–1092; b) R. Jain, T. Bally, P. R. Rablen, *J. Org. Chem.* **2009**, *74*, 4017–4023.
- [48] W. O. George, R. Lewis, in *Handbook of Vibrational Spectroscopy* (Eds.: J. M. Chalmers, P. R. Griffiths), Vol. 3, Wiley, Chichester, **2002**, pp. 1919–1934.
- [49] S. Tsuzuki, A. Fujii, *Phys. Chem. Chem. Phys.* **2008**, *10*, 2584–2594.
- [50] a) T. Steiner, A. M. M. Schreurs, J. A. Kanters, J. Kroon, J. van der Maas, B. Lutz, *J. Mol. Struct.* **1997**, *436–437*, 181–187; b) T. Steiner, A. M. M. Schreurs, M. Lutz, J. Kroon, *New J. Chem.* **2001**, *25*, 174–178; c) T. Alaviuhkola, J. Bobacka, M. Nissinen, K. Rissanen, A. Ivaska, J. Pursiainen, *Chem. Eur. J.* **2005**, *11*, 2071–2080.
- [51] a) J. A. N. F. Gomes, R. B. Mallion, *Chem. Rev.* **2001**, *101*, 1349–1383; b) G. Merino, T. Heine, G. Seifert, *Chem. Eur. J.* **2004**, *10*, 4367–4371.
- [52] a) P. Hobza, Z. Havlas, *Chem. Rev.* **2000**, *100*, 4253–4264; b) A. Masunov, J. J. Dannenberg, R. H. Contreras, *J. Phys. Chem. A* **2001**, *105*, 4737–4740; c) K. Hermansson, *J. Phys. Chem. A* **2002**, *106*, 4695–4702; d) I. V. Alabugin, M. Manoharan, S. Peabody, F. Weinhold, *J. Am. Chem. Soc.* **2003**, *125*, 5973–5987; e) E. S. Kryachko, in *Hydrogen Bonding–New Insights* (Ed.: S. J. Grabowski), Springer, Dordrecht, **2006**, pp. 293–336; f) A. D. Buckingham, J. E. Del Bene, S. A. C. McDowell, *Chem. Phys. Lett.* **2008**, *463*, 1–10.
- [53] J. Joseph, E. D. Jemmis, *J. Am. Chem. Soc.* **2007**, *129*, 4620–4632.
- [54] E. Arunan, G. R. Desiraju, R. A. Klein, J. Sadlej, S. Scheiner, I. Alkorta, D. C. Clary, R. H. Crabtree, J. J. Dannenberg, P. Hobza, H. G. Kjaergaard, A. C. Legon, B. Mennucci, D. J. Nesbitt, *Pure Appl. Chem.* **2011**, *83*, 1619–1636.
- [55] a) For a comparison of cooperativity in CH \cdots O and in OH \cdots O hydrogen bonds, see: T. Kar, S. Scheiner, *J. Phys. Chem. A* **2004**, *108*, 9161–9168; b) for cooperativity in bifurcated hydrogen bonds, see: R. D. Parra, J. Ohlssen, *J. Phys. Chem. A* **2008**, *112*, 3492–3498.
- [56] A. Y. Li, *J. Mol. Struct.* **2008**, *862*, 21–27.
- [57] N. S. Golubev, G. S. Denisov, S. Macholl, S. N. Smirnov, I. G. Shenderovich, P. M. Tolstoy, *Z. Phys. Chem. (Muenchen Ger.)* **2008**, *222*, 1225–1245.
- [58] Z.-L. Zhou, J. F. W. Keana, *J. Org. Chem.* **1999**, *64*, 3763–3766.
- [59] For example, the photochemistry of quaternary phosphonium salts cannot be understood without considering the nature of the anion and the concentration of the salt (ref. [19]).

Received: December 21, 2012
Revised: June 6, 2013
Published online: ■■■, 0000

Hydrogen Bonds

J. Ammer,* C. Nolte, K. Karaghiosoff,*
S. Thallmair, P. Mayer,
R. de Vivie-Riedle, H. Mayr ■■■■-■■■■

Ion-Pairing of Phosponium Salts in Solution: C–H···Halogen and C–H··· π Hydrogen Bonds



Hydrogen bonds: The ^1H NMR chemical shifts of the $\text{C}(\alpha)\text{-H}$ protons of benzhydryl and benzyl triphenylphosphonium salts in CD_2Cl_2 solution strongly depend on the counter-anions (see graphic). The large downfield shifts result from $\text{C-H}\cdots\text{X}^-$ hydrogen

bonds with the anions X^- , which is confirmed by quantum chemical calculations and by the crystal structures. The BPh_4^- anion forms $\text{C-H}\cdots\text{Ph}$ hydrogen bonds causing upfield shifts of the benzyl protons. IR spectra show red- or blue-shifts depending on X^- .